Nuclear pore complex component MOS7/Nup88 is required for plant innate immunity and nuclear accumulation of defense regulators

Yu Ti Cheng[1,2,*], Marcel Wiermer[1,*], Hugo Germain[1,*], Dongling Bi[4,*], Fang Xu[1,3,4], Ana V. Garcia[5], Lennart Wirthmueller[5], Charles Despres[6], Jane E. Parker[5], Yuelin Zhang[4], and Xin Li[1,2,3,§]

[1] Michael Smith Laboratories, Room 301, 2185 East Mall, University of British Columbia, Vancouver, BC V6T 1Z4, Canada

[2] Genetics Graduate Program, University of British Columbia, Vancouver, British Columbia V6T 1Z3, Canada

[3] Dept. of Botany, Room 3529, 6270 University Blvd., University of British Columbia, Vancouver, BC V6T 1Z4, Canada

[4] National Institute of Biological Sciences, Zhongguancun Life Science Park, 7 Science Park Road, Beijing 102206, People's Republic of China

[5] Department of Plant-Microbe Interactions, Max-Planck Institute for Plant Breeding Research, Carl-von-Linné-Weg 10, 50829 Cologne, Germany

[6] Department of Biological Sciences, Brock University, St. Catherines, Ontario, Canada L2S 3A1

[*] These authors contributed equally to the work described in the manuscript.
[§] For correspondence: xinli@interchange.ubc.ca

Abstract

Plant immune responses depend on dynamic signaling events across the nuclear envelope through nuclear pores. Nuclear accumulation of certain Resistance (R) proteins and downstream signal transducers are critical for their functions. It is not understood how these processes are controlled. Here, we report the identification, cloning and analysis of Arabidopsis *modifier of snc1, 7* (*mos7-1*), a partial loss-of-function mutation that suppresses immune responses conditioned by the auto-activated R protein, snc1. *mos7-1* single mutant plants exhibit defects in basal and R protein-mediated immunity and in systemic acquired resistance, but do not display obvious pleiotropic defects in development, salt tolerance or plant hormone responses. MOS7 is homologous to human and *Drosophila* nucleoporin Nup88 and resides at the nuclear envelope. In animals, Nup88 is required to attenuate nuclear export of activated NF-κB transcription factors, resulting in nuclear accumulation of NF-κB and subsequent activation of immune-responsive gene expression. Our analysis shows that nuclear accumulation of snc1 and the defense signaling components EDS1 and NPR1 is significantly reduced in *mos7-1* plants, while nuclear retention of Histone H3, AtCDC5, HDA19 or TGA2 is unaffected. The data suggest that regulating specifically the nuclear concentrations of certain nuclear defense regulators controls defense outputs.

Introduction

Innate immunity in plants against microbial pathogen infection is a dynamic process that requires stimulus-dependent spatial and temporal action of its defense regulatory components. One of the most effective disease resistance mechanisms is mediated by Resistance (R) proteins. Upon infection, an R protein recognizes a specific pathogen effector (termed Avirulence; Avr protein) and mounts a fast and robust response leading to a local hypersensitive response (HR), a form of programmed cell death to restrict pathogen growth and spread (Jones and Dangl, 2006). Many *R* genes have been cloned and the majority encode proteins containing NB-LRR domains in which the NB is a central Nucleotide Binding site and LRRs are C-terminal Leucine-Rich Repeats. There are two subclasses of NB-LRR proteins, varying according to their N-termini (Martin et al., 2003; Belkhadir et al., 2004; McHale et al., 2006). TIR-NB-LRR-type R proteins carry an N-terminal Toll Interleukin Receptor (TIR) domain while the CC-type has a predicted Coiled Coil domain (also called Leucine Zipper domain) at its N-terminus. These two NB-LRR classes differ in their initial mode of signaling since TIR-NB-LRR proteins activate resistance and cell death through EDS1/PAD4/SAG101 (Enhanced Disease Susceptibility 1; Phytoalexin-Deficient 4; Senescence Associated Gene 101) complexes, whereas CC–NB-LRR proteins commonly utilize NDR1 (Non race-specific Disease Resistance 1) (Century et al., 1997; Aarts et al., 1998; Feys et al., 2005; Wiermer et al., 2005). NDR1 associates with the plasma membrane, while EDS1 interacts with PAD4 and SAG101 in distinct complexes in the cytosol and nucleus (Coppinger et al., 2004; Feys et al., 2005). Downstream of EDS1 and NDR1, pathways converge at the synthesis of the defense hormone salicylic acid (SA), a sufficient and necessary signal for systemic acquired resistance (SAR) (Vernooij et al., 1994). SAR represents systemic responses induced throughout the plant to enhance resistance. NPR1 (Nonexpressor of *PR* genes 1) is a key positive regulator of SAR whose monomerization and nuclear accumulation is essential for its activity in stimulating defense gene expression (Cao et al., 1997; Mou et al., 2003; Tada et al., 2008).

The detailed biochemical functions of NB-LRR proteins have started to emerge in recent years. They are normally under tight negative control. Upon infection, the release of repression seems to be the driving force for the resistance responses. For example, studies on the *Arabidopsis*

defense modulator RIN4 revealed that it negatively regulates two different CC-NB-LRR-type R proteins, RPM1 and RPS2 (Mackey et al., 2002; Axtell and Staskawicz, 2003; Mackey et al., 2003; Kim et al., 2005). Although most NB-LRR proteins are predicted to be cytosolic (Jones and Dangl, 2006), MLA1 and MLA6 belonging to the CC-NB-LRR class localize partially to and function inside the nucleus (Shen et al., 2007). Upon infection, recognition of its cognate fungal effector induces MLA interaction with repressive WRKY transcription factors, leading to deregulation of downstream defense gene expression. Also, the TIR-type NB-LRR proteins, N in tobacco and RPS4 in *Arabidopsis*, need to accumulate in nuclei to function (Burch-Smith et al., 2007; Wirthmueller et al., 2007). These recent discoveries suggest there may be a general requirement for nuclear localization of R proteins or their downstream signaling components in R-mediated resistance.

Previous studies of MOS3 (Modifier of *snc1*, 3; Zhang and Li 2005), MOS6 (Palma et al. 2005) and RanGAP2 (Sacco et al., 2007; Tameling and Baulcombe, 2007) reveal the importance of two nucleocytoplasmic trafficking pathways in plant innate immunity - mRNA export and Nuclear Localization Signal (NLS)-dependent nuclear protein import. It is not known whether other nucleocytoplasmic trafficking machineries, such as those governing nuclear protein export pathways, contribute to plant disease resistance. MOS3/AtNUP96/SAR3 is required for mRNA export (Dong et al., 2006; Parry et al., 2006) and mutations in *MOS3* confer enhanced susceptibility to both virulent and avirulent pathogens. Also, mutations in *MOS6*, an Importin α homolog responsible for importing proteins with an NLS to the nucleus, compromise plant defense against pathogen infection. RanGAP2, another component of the protein nuclear import machinery, interacts with the NB-LRR protein Rx, and silencing of *RanGap2* impairs Rx resistance (Sacco et al., 2007; Tameling and Baulcombe, 2007).

Both MOS3 (Zhang and Li 2005) and MOS6 (Palma et al. 2005) were identified in a forward genetic screen for modifiers of *snc1* (*mos*) aimed at finding components that function downstream of R protein activation. In *snc1* (*suppressor of npr1-1, constitutive 1*), a point mutation resulting in an E to K change in the linker region between the NB and LRR of an *RPP4* homolog, renders this TIR-type R protein constitutively active without pathogen recognition (Zhang et al., 2003a). As a consequence, *snc1* mutant plants are dwarf, accumulate high levels of

SA, and exhibit enhanced disease resistance against virulent pathogens (Li et al., 2001; Zhang et al., 2003a). As a TIR-NB-LRR protein, *snc1* was accordingly found to be fully dependent on EDS1/PAD4, whose nucleocytoplasmic partitioning and complex formation is probably under tight control (Feys et al., 2005; Wiermer et al., 2005).

In this study, we report the isolation, positional cloning and detailed functional analysis of *MOS7.* A partial loss-of-function mutation, *mos7-1*, suppresses *snc1* autoimmune phenotypes, while complete loss of *MOS7* in *mos7-2* and *mos7-3* mutants causes lethality. In the *mos7-1* single mutant, basal defense against virulent pathogens, local resistance conditioned by several TIR- and CC-type NB-LRR R proteins and SAR responses are impaired. *MOS7* encodes a protein homologous to the human Nup88 nucleoporin. In *Drosophila* and human, mutations in Nup88 enhance CRM1 (Chromosomal Region Maintenance 1; also named Exportin 1; XPO1)-dependent nuclear export of activated NF-κB transcription factors (Roth et al., 2003; Xylourgidis et al., 2006). In this study, we establish that MOS7 is required for appropriate nuclear accumulation of the auto-activated R protein snc1, as well as the downstream defense signaling components, EDS1 and NPR1.

Results

Identification of the *mos7-1* mutant

The *modifier of snc1, 7* (*mos7-1*) mutant was identified from a MOS (modifier of *snc1*) forward genetic screen with fast neutrons, as described earlier (Zhang and Li, 2005). *snc1* plants have a stunted stature and curly leaves due to constitutive defense activation (Zhang et al., 2003a). The suppressor screen was designed to search for mutants that resemble wild-type morphology and abolish constitutive pathogen resistance in *snc1*. *mos7-1 snc1* double mutant plants are larger than *snc1* plants (Figure 1A). In *snc1* plants, several *Pathogenesis Related* (*PR*) defense marker genes are constitutively expressed. Analysis using RT-PCR showed that *PR-1* and *PR-2* expression was suppressed in *mos7-1 snc1* when compared to *snc1* (Figure 1B).

snc1 plants exhibit enhanced resistance against virulent pathogens including the bacterium *Pseudomonas syringae* pv *maculicola* (*P.s.m.*) ES4326 and the oomycete pathogen

Hyaloperonospora arabidopsidis (*H.a.*; previously named *Peronospora parasitica* or *Hyaloperonospora parasitica*) Noco2 (Zhang et al., 2003a). To determine whether *mos7-1* mutation alters the *snc1* autoimmune response, we inoculated *mos7-1 snc1* double mutant plants with these pathogens. As shown in Figure 1C and 1D, *mos7-1 snc1* double mutants had lost enhanced resistance to both pathogens. Bacterial growth in *mos7-1 snc1* was even higher than in wild-type plants (Figure 1D).

SA levels are elevated in the *snc1* mutant (Li et al., 2001). To determine whether *mos7-1* affects SA accumulation in *snc1*, SA was extracted and measured from *mos7-1 snc1* plants. As shown in Figure 1E and 1F, levels of free and total SA in *mos7-1 snc1* were similar to those of wild-type plants and approximately 4-fold lower than in *snc1*. Therefore, *mos7-1* fully suppresses all known autoimmune phenotypes of *snc1*.

When *mos7-1 snc1* was backcrossed with *snc1*, the F_1 progeny had a *snc1* morphology. Of 40 F_2 plants, 28 were *snc1*-like whereas 12 were wild type-like. The 1:3 wild type to *snc1*-like ratio ($\chi^2 = 0.53$; $p>0.1$) together with the F_1 phenotype are consistent with *mos7-1* being a single, recessive nuclear mutation.

Map-based cloning of *mos7-1*

A positional cloning approach was used to identify the mutation in *mos7-1* leading to the suppression of *snc1*. To map *mos7-1*, *mos7-1 snc1* in Columbia (Col) ecotype was crossed with Landsberg *erecta* (Ler) containing the introgressed *snc1* mutation, Ler-*snc1* (Zhang and Li, 2005). Linkage analysis was carried out on 24 F_2 plants that had lost the *snc1* morphology. The *mos7-1* locus was found to have linkage with markers on the top arm of chromosome 5 that unfortunately was not introgressed from Ler to Ler-*snc1*. Therefore, a population of 1056 F_3 plants was generated for fine mapping from F_2 progeny that were homozygous for *snc1* and heterozygous for *mos7-1* from another cross between *mos7-1 snc1* and Ler. The *mos7-1* mutation was narrowed to the region between markers MOP10 and MJJ3 on chromosome 5 (Figure 2A). To identify the molecular lesion in *mos7-1*, a set of overlapping PCR fragments covering coding sequences in this region were amplified from *mos7-1 snc1* and sequenced. Comparing sequences from the mutant with the *Arabidopsis* genome sequence revealed a 12 base pair deletion in the

fourth exon of *At5g05680* (Figure 2C) that leads to an in-frame deletion of four amino acids at the N-terminus of MOS7 (Supplementary Figure S1). BLAST analysis showed that MOS7 is related to human Nup88 and *Drosophila* Mbo (members only) proteins (Figure S1). MOS7 is the only Nup88 homolog in *Arabidopsis*. The homology between MOS7 and Nup88 and Mbo is throughout the entire length of the protein.

To confirm that *MOS7* is *At5g05680*, a wild-type copy of *At5g05680* under the control of its own promoter was transformed into *mos7-1 snc1*. Among 12 T_1 transgenic plants obtained, all displayed *snc1*-like morphology (Figure 2D). Progeny of T_1 plants carrying the *MOS7* transgene were tested for resistance against *H.a.* Noco2. Constitutive resistance to *H.a.* Noco2 was restored in the transgenic plants (Figure 2E), indicating that *At5g05680* is able to complement *mos7-1*, and that *MOS7* is *At5g05680*. Two additional mutant alleles of *MOS7* were obtained from the Arabidopsis Biological Resource Center (ABRC). *mos7-2* (SALK_129301) contains a T-DNA insertion in the third intron and *mos7-3* (SALK_085349) has a T-DNA inserted in the sixth exon of *MOS7* (Figure 2B). We were unable to identify plants that are homozygous for either *mos7-2* or *mos7-3* from more than 200 progeny of plants heterozygous for the mutations (data not shown), indicating that null mutations of *MOS7* are lethal. This is consistent with the lethality phenotype of null *mbo* alleles in *Drosophila* (Uv et al., 2000). The viability of *mos7-1* suggests that it is a partial loss-of-function allele of *MOS7*.

To obtain a *mos7-1* single mutant, *mos7-1 snc1* was crossed with wild type Col plants. Lines homozygous for *mos7-1* and wild type for *SNC1* were selected as the *mos7-1* single mutant. We tested whether *mos7-1* and *mos7-2* or *mos7-3* are allelic by crossing plants heterozygous for *mos7-2* or *mos7-3* with *mos7-1*. *mos7-1*/*mos7-2* plants were identified by PCR and were found to support higher bacterial growth than wild type (Supplementary Figure S2), indicating that *mos7-1* and *mos7-2* do not complement each other and therefore carry mutations in the same gene. Similar results were obtained with crosses between *mos7-1* and *mos7-3* (data not shown).

mos7-1 single mutant plants exhibit enhanced disease susceptibility

To test whether *MOS7* contributes to basal defense against virulent pathogens, *mos7-1* plants were challenged with *P.s.m.* ES4326 at a concentration of OD_{600} = 0.0001. Wild type plants

usually develop no disease symptoms at this low dose; however, subtle disease symptoms were observed on *mos7-1* plants 3d after inoculation. When bacterial growth was determined, approximately 10-fold more bacteria accumulated in *mos7-1* than in wild-type leaves (Figure 3A). Therefore, *MOS7* contributes to basal resistance.

MOS7 is required for resistance mediated by multiple R proteins

To determine whether MOS7 is involved in resistance mediated by other TIR-NB-LRR R proteins, we challenged the *mos7-1* single mutant with *H.a.* Emwa1 and *P.s.tomato* DC3000 carrying *avrRps4* that are recognized, respectively by RPP4 (van der Biezen et al., 2002) and RPS4 (Hinsch and Staskawicz, 1996). As shown in Figure 3B and 3C, the *mos7-1* mutation markedly reduced resistance mediated by RPP4. By contrast, RPS4 resistance was only slightly compromised.

We then tested whether resistance mediated by the CC-NB-LRR-type R protein is also impaired in *mos7-1* by inoculating plants with *P.s.m.* ES4326 carrying *avrB* or *P.s.t.* DC3000 carrying *avrPphB* that encode effector proteins recognized, respectively by RPM1 (Grant et al., 1995) and RPS5 (Simonich and Innes, 1995). The *mos7-1* mutant supported approximately 30-fold more bacterial growth compared to wild-type plants when challenged with *P.s.m.* ES4326 carrying *avrB* (Figure 3D). Also, *mos7-1* was highly susceptible to *P.s.t.* DC3000 carrying *avrPphB*, the extent of bacterial growth being the same as in susceptible *ndr1* plants (Figure 3E). These data show that *mos7-1* compromises resistance mediated by both TIR- and CC-NB-LRR proteins, although the degree of its effect varies depending on the R protein tested.

mos7-1 is compromised in systemic acquired resistance

Initiation of local R protein-mediated resistance primes uninfected tissues against subsequent infections by a broad range of pathogens, a process termed systemic acquired resistance (SAR). As a result, the entire plant becomes more resistant to secondary infections (Durrant and Dong, 2004). To test whether SAR is affected in *mos7-1* plants, we first treated leaves locally with *P.s.m.* ES4326 expressing *avrB* at a density of OD_{600} = 0.2 to trigger an HR. A high dose of virulent *P.s.m.* ES4326 (OD_{600} = 0.001) was then infiltrated into the distal leaves 24 h after SAR induction. Wild type plants showed a significant decrease in bacterial growth in *avrB* pretreated

plants compared to mock-inoculated ones. By contrast, leaves of *mos7-1* supported bacterial growth in systemic leaves of both *avrB* pre-treated and untreated plants that was similar to the SAR-defective *npr1-1* mutant (Figure 4A). Therefore, the SAR response is abolished in *mos7-1*. A defect in SAR was also reflected by the inability of *mos7-1* to boost *PR-1* expression in systemic tissue after local *avrB* induction (Figure 4B).

In SA-mediated defense, *npr1-1* and *tga2 tga5 tga6* triple mutants were the only genotypes reported to be sensitive to high concentrations of SA (Cao et al., 1997; Zhang et al., 2003b). To determine whether *mos7-1* plants also have altered responsiveness to high SA, *mos7-1* seeds were plated on MS medium containing 0.2 mM SA. Similar to *npr1-1*, *mos7-1* plants were highly sensitive to SA at an early stage of development (Supplementary Figure S3). Notably, whereas *npr1-1* plants remained bleached on high SA plates, *mos7-1* plants slowly recovered after 5 days and eventually restored a wild type-like appearance (Supplementary Figure 3).

***mos7-1* plants do not exhibit defects in salt tolerance, ethylene and auxin responses**

No obvious developmental defects were observed in *mos7-1* although mutant plants are slightly smaller than wild type. Due to the lethality of its null alleles and pleiotropic phenotypes of reported Nup mutants, such as *mos3* and *nup160* in *Arabidopsis*, we investigated whether *mos7-1* has other abiotic response or hormonal defects. As shown in Supplementary Figure 4, *mos7-1* plants tolerate salt stress to the same level as wild type. Also, no altered ethylene or auxin responses were observed in *mos7-1* seedlings (Supplementary Figure 5A and 5B).

MOS7 localizes to the nuclear rim

In order to explore the roles of MOS7 in plant innate immunity further, we investigated its subcellular localization. Initially we used the native promoter of *MOS7* to drive expression of MOS7 with Green Fluorescent Protein (GFP) fused to its C-terminus. Although *MOS7-GFP* expressed under the native promoter complemented the *mos7-1* mutation (data not shown), we did not observe any green fluorescence using confocal fluorescence microscopy, probably due to low abundance of the fusion protein. A construct containing *MOS7* fused to a C-terminal GFP tag under the control of the constitutive *35S* promoter was then made and transformed into the *mos7-1 snc1* mutant. A green fluorescence signal was observed at the nuclear rim (Figure 5A and

5B). The nuclear rim localization was observed in all cell types examined, including root cells (Figure 5A and 5B) and leaf pavement cells (Figure 5A). Concentration of GFP signal at the nuclear envelope is consistent with MOS7 being a member of the nuclear pore complex (NPC), as predicted by BLAST. The *MOS7-GFP* transgene not only complemented the morphological phenotypes of *mos7-1 snc1* (Figure 5C), but also restored a constitutive defense response against virulent *H.a.* Noco2 (Figure 5D), suggesting that the MOS7-GFP fusion protein localizes correctly inside the cell.

Since *mos7-1* is a partial loss-of-function allele of *MOS7*, we investigated whether *mos7-1* mutation affected *MOS7* expression or protein subcellular localization. No difference in *MOS7* gene expression was observed between *mos7-1* and the wild type (data not shown). mos7-1-GFP localizes to the nuclear rim as does wild type MOS7 protein (Supplementary Figure 6), indicating that *mos7-1* phenotypes are not caused by mis-expression or mis-localization of the nucleoporin.

NES-mediated nuclear protein export is enhanced in *mos7-1*

In fruit fly and human cells, the function of the MOS7 homolog Nup88 is to anchor Nup214 and CRM1 at the nuclear envelop to attenuate NES/CRM-mediated nuclear export (Roth et al., 2003; Bernad et al., 2004; Xylourgidis et al., 2006). Mutations or depletion of Nup88 in animals lead to increased nuclear export of NF-κB transcription factors (Uv et al., 2000; Xylourgidis et al., 2006; Takahashi et al., 2008). In plants, CRM1-like transport is mediated by AtXPO1 (Haasen et al., 1999), a protein with homology to human CRM1.

To test whether *mos7-1* also affects NES-mediated nuclear protein export, we took advantage of an established nuclear export/import assay system (Haasen et al., 1999). Here, the cytosolic protein chalcone synthase (CHS) is fused to the NLS from the SV40 large antigen together with the leucine-rich NES from the HIV-1 Rev protein and GFP. Localization of the recombinant protein (GFP-NLS-CHS-NES) can be monitored by microscopy after transfection of protoplasts. When GFP-NLS-CHS-NES was transfected into wild type Col mesophyll protoplasts, a nucleo-cytoplasmic localization was observed (Supplementary Figure 7), with 12.53±6.63% of the GFP signal in the nucleus. When the same construct was transformed in *mos7-1* protoplasts, nuclear

accumulation was almost not observed (Supplementary Figure 7). Significantly less (3.56±2.23%; $p<0.001$) of the GFP signal is detected in the nucleus. As a control we used the same construct in which the NLS was mutated to a non-functional form (GFP-NLS_{mut}-CHS-NES). In both wild type and *mos7-1*, localization of this protein was mostly cytosolic (Supplementary Figure 7). When only CHS protein fused to GFP was transformed into the same genotypes, weak nuclear and cytosolic localizations were observed (Supplementary Figure 7). These results indicate that *mos7-1* cells fail to retain an NES-containing nuclear protein in the nucleus, whereas a protein that does not have an NES (GFP-CHS) is unaffected (Supplementary Figure 7). The data support an activity of plant Nup88/MOS7 in CRM1/Exportin-mediated nuclear protein export. As its homologs in animal systems, mutation in *mos7-1* enhances NES-mediated nuclear export, causing reduced nuclear retention of nuclear proteins (Supplementary Figure 7).

Nuclear accumulation of snc1 Resistance protein is reduced in *mos7-1*

Recent studies on tobacco N and *Arabidopsis* RPS4, two TIR-type NB-LRR proteins revealed that both are present in the cytoplasm and nucleus and that their nuclear pools are important for triggering immune responses (Burch-Smith et al., 2007; Wirthmueller et al., 2007). However, the mechanism by which their partitioning between the cellular compartments is controlled remains elusive. The TIR-type R protein SNC1 contains a predicted NLS and two NES motifs. Since *mos7-1* was identified as a genetic suppressor of *snc1*, one obvious candidate protein whose cellular distribution could be affected by *mos7-1* is snc1. We therefore made a *snc1-GFP* fusion gene construct driven by its own promoter and transformed this into *snc1-r3* that contains a deletion of the entire *RPP4* cluster. *snc1-r3* was identified as a *snc1* revertant allele from the MOS screen (Zhang et al., 2003a) and was used in this study to avoid potential interference by endogenous SNC1-related proteins. Of many transgenic plants obtained, we were unable to find lines that consistently exhibit green fluorescence, probably due to low levels of the fusion protein. We selected one line with a single insertion site that exhibited an *snc1*-like morphology, and crossed it with *mos7-1* to generate a *mos7-1 snc1-r3* line expressing the identical *snc1-GFP* transgene. Homozygous *snc1-GFP* transgenic plants were much smaller than *snc1* plants, probably due to overexpression of the transgene in this particular line. *mos7-1* partially suppressed the morphological phenotypes of *snc1-GFP* in *snc1-r3* (Figure 6A) and constitutive

defense against virulent *H.a.* Noco2 (Figure 6B). Western blot analysis showed that total snc1-GFP levels were similar in *snc1-r3* and *mos7-1 snc1-r3* (Figure 6C). Further fractionation revealed that snc1-GFP was present in both the nuclear-depleted and nuclear fraction (Figure 6D). When band intensities were measured by Quantity One 4.6.1 software (BioRad), we estimated from repeated experiments that the majority of snc1 protein accumulates in the cytoplasmic compartment with 5.6-11.5% in the nucleus (Figure 6D). In *mos7-1*, there was a significant increase of snc1-GFP protein in the cytoplasm, whereas the nuclear pool of snc1-GFP was reduced (Figure 6D), ranging between 2.5 and 2.9% of total snc1 protein. We reasoned that the altered cellular distribution of snc1-GFP likely contributes to the *snc1*-suppressing phenotype of *mos7-1*.

In *Drosophila* and human, mutations in Nup88 enhance NES-mediated nuclear export (Roth et al., 2003; Xylourgidis et al., 2006). We further tested whether adding an NES to snc1-GFP would affect snc1-mediated resistance. When a construct expressing snc1-GFP-NES driven by its native promoter was transformed into wild type Col, none of the T1 transgenic plants showed *snc1*-like morphology, while 61% of the transgenic plants carrying the control *snc1-GFP* transgene in Col showed *snc1*-like morphology. The numbers here support that snc1 nuclear localization is probably critical for its autoimmunity. Enhancing nuclear export of snc1-GFP results in reduced autoimmunity, a similar effect as observed in *mos7-1*.

Nuclear accumulation of NPR1 is reduced in *mos7-1*

In *Drosophila*, the MOS7 homolog DNup88 affects an immune response against bacterial infection through nuclear retention of master immune regulators of the NF-κB family (Uv et al., 2000; Xylourgidis et al., 2006). Upon infection, the I-κB homolog Cactus becomes degraded, allowing the Rel/NF-κB proteins Dorsal and Dif to translocate to the nucleus and activate gene expression. During this process, DNup88 attenuates CRM1-mediated nuclear export of Dorsal and Dif, leading to their nuclear accumulation, whereas *nup88* mutant larvae exhibit enhanced nuclear export of the Rel/NF-κB proteins and fail to activate an immune response (Uv et al., 2000; Roth et al., 2003; Xylourgidis et al., 2006).

The plant defense regulator NPR1 controls basal resistance and SAR downstream of the defense hormone SA, and displays a somewhat analogous pattern of activation as NF-κB. Using *35S* promoter-driven *NPR1-GFP*, it was shown that under non-inducing conditions NPR1 is sequestered in the cytoplasm as an oligomeric complex (Mou et al., 2003; Tada et al., 2008). Upon SA application, increased SA levels result in a change of the cellular redox state which in turn leads to monomerization of NPR1, allowing it to translocate from the cytosol to the nucleus to regulate downstream *PR* gene expression. The SAR defect observed in *mos7-1* mutant plants (Figure 4A, 4B, and Supplementary Figure 3) prompted us to investigate the contribution of MOS7 to NPR1 nuclear accumulation.

To avoid artifacts that can result from overexpression from the 35S promoter, we constructed an *NPR1-GFP* fusion gene driven by its native promoter. When the *NPR1-GFP* transgene was transformed into the null *npr1-3* mutant, none of the transgenic lines consistently exhibit green fluorescence even upon SAR induction, suggesting that levels of the fusion protein in the transgenic plants are very low. We selected one line that carried a single transgene insertion and complemented fully all *npr1* phenotypes (Supplementary Figure 8), suggesting that NPR1-GFP expressed by its own promoter functions similarly to wild type NPR1 protein. The *NPR1-GFP* transgenic line was then crossed with *mos7-1* to create a *mos7-1 npr1-3* double mutant expressing the same NPR1-GFP protein. As shown in Figure 7A, NPR1 total protein levels increased markedly in both wild type and the *mos7-1* mutant upon SAR induction by spraying plants with the SA analog 2,6-dichloroisonicotinic acid (INA). Lower amounts of NPR1 protein accumulated in *mos7-1* before and after SAR induction compared to wild type. No differences in *NPR1* transcript abundance were observed between uninduced *npr1-3* and *mos7-1 npr1-3* tissues determined by semi-quantitative RT-PCR (Figure 7B), suggesting that reduced NPR1 accumulation in *mos7-1* likely results from decreased protein synthesis or stability rather than reduced transcription.

We further investigated the cellular distribution of NPR1-GFP in *mos7-1* before and after INA induction by comparing NPR1-GFP levels in nuclear and nuclei-depleted protein extracts of untreated and INA-induced tissues. As shown in Figure 7C, lower levels of NPR1-GFP accumulated in nuclei of both healthy and INA-induced *mos7-1* plants than in wild type. In

contrast to the preferential depletion of nuclear snc1 in *mos7-1* tissues, lower amounts of NPR1-GFP were also observed in nuclei-depleted (cytosolic) extracts of INA-treated *mos7-1* compared to wild type (Figure 7C). Since *mos7-1* plants exhibit a SAR defect and nuclear accumulation of NPR1 is required for SAR induction, these data suggest that NPR1 may not be able to attain sufficient abundance in the nucleus for activation of SAR in *mos7-1*.

It is notable that NPR1-GFP expressed under its native promoter was detected in the nucleus of uninduced tissues (Figure 7C). A similar expression pattern was observed in multiple independent *NPR1-GFP* transgenic lines (data not shown). This partitioning contrasts with data derived from *NPR1-GFP* expressed under control of the *35S* constitutive promoter that showed a cytoplasmic localization of NPR1 without SAR induction (Mou et al., 2003). To rule out the possibility that unchallenged plants were already stressed, causing increased nuclear translocation of NPR1-GFP, we analyzed the expression of the SAR marker gene *PR-1* in the same uninduced tissues from which nuclear extracts were generated. No *PR-1* transcripts were detected in uninduced tissues whereas strong expression was detected after INA-induction (data not shown), suggesting that the observed nuclear pool of NPR1 represents its uninduced state. These data suggest that NPR1 is present in the nucleus of both uninduced and INA-induced tissues.

EDS1 nuclear accumulation is reduced in *mos7-1*

Another key plant immune regulator known to localize to both cytosol and nucleus is EDS1 (Feys et al., 2005). We investigated whether accumulation and cellular distribution of native EDS1 is affected by *mos7-1*. As with NPR1, EDS1 total protein was reduced in *mos7-1* mutant plants compared to Col wild-type (Figure 8A), although wild-type and *mos7-1* have comparable *EDS1* transcript levels (Figure 8B). In *mos7-1*, the ratio of EDS1 distributing in the cytosol and nucleus was not strongly affected. However, overall lower accumulation of EDS1 resulted in only very low levels being detected in *mos7-1* nuclei (Figure 8C). We conclude that MOS7 is also necessary for EDS1 protein accumulation in the nucleus. The effect of *mos7-1* on EDS1 nuclear accumulation may also contribute to the ability of *mos7-1* to suppress *snc1*.

Nuclear accumulation of HDA19, AtCDC5 and TGA2 is not affected in *mos7-1*

One enigma to *mos7-1* is its specificity. Lethality of its null alleles indicates that wild type MOS7 is probably required for general nuclear export. While *mos7-1* appeared not to exhibit pleiotropic phenotypes, we could not rule out a global effect on protein export. To test this, we fractionated proteins from *mos7-1* and wild type and examined the localization and relative protein abundance of the known nuclear proteins AtCDC5, HDA19 and TGA2 using respective antibodies. AtCDC5 is a myb-like transcription factor belonging to a nuclear MOS4-accociated complex (MAC; Palma et al., 2007). HDA19 is a histone deacetylase and TGA2 is a transcription factor that interacts with NPR1 (Zhang et al., 1999). As shown in Figure 9, nuclear accumulation of these proteins (as well as histone H3) is unaffected in *mos7-1*. These data suggest that the defects we observe in *mos7-1* in nuclear retention of snc1, NPR1 and EDS1 are rather selective.

Discussion

Several recent lines of evidence suggest that nucleocytoplasmic trafficking pathways play important roles in plant innate immunity through dynamic partitioning of signaling regulators between the nucleus and cytosol. Studies of MOS3/SAR3 indicate that mRNA export, regulated by nucleoporins of the Nup107-160 complex, is required for both basal defense and R protein-mediated resistance (Zhang and Li, 2005; Dong et al., 2006; Parry et al., 2006). Also, a requirement for MOS6 and RanGAP2 in R protein-triggered resistance points to import to the nucleus of protein regulators that have NLSs as an important process in plant immunity (Palma et al., 2005; Sacco et al., 2007; Tameling and Baulcombe, 2007). However, contributions of other nucleocytoplasmic trafficking pathways or components controlling nuclear protein export and retention, are unknown. In this study, we identified *mos7-1* as a genetic suppressor of the autoimmune mutant *snc1*. We isolated the *MOS7* gene and found it to encode a plant homolog of human and *Drosophila* nucleoporin 88 (Nup88). Our analysis reveals that MOS7 contributes to several aspects of plant immunity. Importantly, resistance defects of *mos7-1* mutants correlate specifically with reduced nuclear accumulation of the auto-activated TIR-NB-LRR immune receptor, snc1. Nuclear pools of the downstream signaling components NPR1 and EDS1 are also strongly depleted in *mos7-1*, although unlike snc1, reduced abundance in nuclei appears to reflect lower total steady state levels of these defense regulators.

While only limited studies have been carried out on nucleoporins in plants, nuclear pore complexes seem to be conserved among eukaryotes, in both structure and functionality (Terry et al., 2007). For example, Nup107-160 complexes in yeast and animals are critical for mRNA export (Dockendorff et al., 1997; Emtage et al., 1997). In *Arabidopsis*, mutations in homologs of Nup160 and Nup96, both belonging to the corresponding Nup107-160 complex, similarly affect mRNA export (Dong et al., 2006; Parry et al., 2006). Mutations in *Arabidopsis MOS3/Nup96/SAR3* partially disable innate immunity (Zhang and Li, 2005). In mice, although a complete knockout of *Nup96* causes lethality, knockdown of Nup96 exhibits defects in both innate and adaptive immunity (Faria et al., 2006). Our studies on MOS7 suggest that the function of Nup88 is also conserved between plants and animals since Nup88s in *Drosophila* and human are critical for the regulation of innate immunity. Consistent with this idea, MOS7-GFP fusion protein resides mainly at the nuclear rim (Figure 5A and 5B). In animals, Nup88 interacts directly with CAN/Nup214 and Nup358/RanBP2. The major function of Nup88 is to anchor Nup214 and CRM1 on the nuclear envelope to attenuate nuclear export sequence (NES)-mediated nuclear export (Roth et al., 2003; Bernad et al., 2004; Xylourgidis et al., 2006). Partial loss-of-function mutations in *Drosophila mbo* or depletion of mammalian Nup88 lead to increased nuclear export, resulting, respectively, in reduced retention of *Drosophila* Rel protein Dorsal and NF-κB (Uv et al., 2000; Xylourgidis et al., 2006; Takahashi et al., 2008). Our analysis suggests that nuclear accumulation of snc1, NPR1 and EDS1 is controlled in part by MOS7. *mos7-1* affects nuclear levels of all three proteins as well as those of a synthetic GFP-NLS-CHS-NES, indicating that like its homologs in animals, MOS7 probably functions in restricting NES-mediated nuclear export in plants.

Previous studies revealed nuclear pools of the plant NB-LRR proteins MLA, N and RPS4 and that their nuclear accumulation is required for disease resistance (Burch-Smith et al., 2007; Shen et al., 2007; Wirthmueller et al., 2007). Future nuclear partitioning analysis of wild type SNC1 should resolve whether SNC1 has nuclear activity, and if so whether the nuclear activity of SNC1 is essential for activation of defense responses. We find that snc1 (an auto-activated NB-LRR protein) localizes to both the cytosol and the nucleus. Nuclear accumulation of snc1 is disproportionately reduced in *mos7-1* and adding an NES to snc1-GFP abolishes its

autoimmunity, suggesting that MOS7/Nup88 promoting retention of snc1 in the nucleus is a critical process in defense activation. It is notable that resistance mediated both by CC- (RPM1 and RPS5) and TIR-NB-LRR (RPP4) proteins, was strongly compromised in *mos7-1*, suggesting that some R proteins may require MOS7 for nuclear retention. Whether these tested NB-LRR receptors have a nuclear activity remains to be characterized. On the other hand, RPS4 resistance was only marginally compromised in *mos7-1*, and no detectable change in RPS4 nuclear accumulation was observed in *mos7-1* (Supplementary Figure 9). Further analysis should establish whether regulation of nucleocytoplasmic partitioning of NB-LRR proteins by MOS7 is a general phenomenon or whether MOS7 is selective for certain R proteins depending on their intracellular abundance, spatial dynamics and activities.

One striking phenotype of *mos7-1* is its defect in SAR. Similar to the SAR-deficient *npr1* mutants, *mos7-1* plants had reduced *PR* gene expression and systemic resistance after SAR induction, and exhibited reduced tolerance to high levels of SA. Since NPR1 nuclear accumulation is essential for SAR and lower NPR1 levels were observed in nuclei of *mos7-1* plants after SAR induction, the SAR defects in *mos7-1* are likely caused by the reduced nuclear NPR1 pool. Nuclear accumulation of EDS1 was also reduced in *mos7-1*. Reducing the nuclear EDS1 pool partially disables plant defenses (AV Garcia and JE Parker, unpublished) and therefore lower amounts of nuclear EDS1 probably contribute to the enhanced disease susceptibility phenotype of *mos7-1*. For both EDS1 and NPR1, there is a general decrease in protein accumulation in both non-nuclear and nuclear compartments of the *mos7-1* mutant. Thus, the influence of *mos7-1* on these proteins is different to its effect on snc1. The data support selective retention of snc1 inside the nucleus by MOS7. By contrast, MOS7 may act more indirectly on EDS1 and NPR1. One scenario is that lower cellular accumulation of EDS1 and NPR1 reflects an indirect influence of MOS7 by lowering basal resistance and thus the flux through various positive feedback loops (Feys et al., 2001; Shah, 2003). However, *mos7-1* did not affect expression of *NPR1* or *EDS1* mRNAs, suggesting that such feedback mechanisms are not operating at the transcriptional level. Alternatively, MOS7 may act directly on these proteins but they are subject to increased degradation after being exported from the nucleus, thereby reducing the amount in a cytosolic pool available for nuclear import.

Plant defense responses rely on dynamic translocation of signaling components across the nuclear envelope and nucleocytoplasmic trafficking might constitute a central regulatory node for the integration of distinct signaling pathways. Although *mos7-1* exhibits strong immunity defects, overexpression of *MOS7* did not lead to enhanced disease resistance (data not shown), supporting the notion that MOS7 itself is probably not a rate-limiting defense signaling component. The identification of MOS7 reveals how the nuclear protein export pathway contributes to cellular innate immune responses and provides us with a system to test the relevance of different cellular compartments in plant-pathogen recognition and defense activation.

Material and methods

Plant growth conditions and mutant phenotypic characterization

All plants were grown at 22°C under 16h light/8hr night or 10 h light/14h night cycles. The *snc1* suppressor screen was described previously (Zhang and Li, 2005). Gene expression analysis was done by extracting RNA from 3-week-old plate-grown or 4-week-old soil-grown plants using the Total RNA kit (Ambion, Austin, TX). The extracted RNA was then reverse transcribed using the RT-for-PCR kit (Clonetech, Palo Alto, CA) or the SuperScript™ II RNase H- Reverse Transcriptase (Invitrogen). Real-time PCR was performed using the QuantiTect SYBR Green PCR kit (Qiagen, Valencia, CA) and the expression levels of *Actin1*, *PR1*, and *PR2* were determined as described previously (Zhang et al., 2003a). Infection experiments with *P. syringae* and *H. arabidopsidis* (previously *H. parasitica*) were performed as described (Li et al., 2001). Endogenous SA levels were determined as described in Li et al. (1999).

Map-based cloning of *mos7-1*

Positional cloning of *mos7-1* was carried out according to procedures described in Zhang and Li (2005). The markers used to map *mos7-1* were derived from insertion-deletion (InDel) polymorphisms (Supplementary Table 1) identified from the genomic sequences of Col and Ler ecotypes provided by Monsanto on the TAIR homepage (Jander et al., 2002).

Construction of plasmids

The construct used to complement the *mos7-1* mutation was generated by PCR amplifying a genomic fragment containing the *MOS7* coding region and its promoter 1.1 kb upstream of the ATG start codon. The primers MOS7 pro-F (ccaatacacaaaatactctggc) and MOS7-3' (cgcGGATCCtgcgtccctgttacagtga) were used for PCR, and the fragment was subsequently cloned into *pGreen0229* (Hellens et al., 2000) to obtain *pG229-MOS7* for complementation analysis. To generate *35S*-driven *MOS7-GFP* construct, full-length *At5g05680* cDNA lacking a stop codon was cloned into the *pBS-GFP5* vector with *GFP* in-frame at the C terminus (Haseloff et al., 1997). The resulting *MOS7-GFP* fusion construct was subsequently excised and cloned into *pBI1.4* containing the *35S* promoter to obtain *pBI-MOS7-GFP*. *NPR1-GFP* construct was generated by PCR amplifying *NPR1* cDNA without a stop codon and a 1.6kb genomic region

upstream of the *NPR1* ATG start codon. These two fragments were subsequently cloned into a modified *pGreen0229* vector that has a sequence encoding *GFP* in-frame at the C terminus. To generate *promSNC1-snc1-GFP*, *pG229-snc1* (Zhang et al., 2003a) lacking a stop codon was used as the template for PCR amplification. The amplified fragment was subsequently cloned into *pGreen0229-GFP* vector with *GFP* in-frame at the C-terminus. All constructs were sequenced to ensure accuracy in PCR and cloning. All constructs were transformed into designated genotypes using the floral-dip method (Clough and Bent, 1998) to generate transgenic lines for subsequent analysis.

Systemic acquired resistance experiments

The infection experiment used to test SAR was performed as described in Cao et al. (1994) with minor modifications. In brief, two leaves of each 5-week-old soil-grown plant were infiltrated with *P.s.m.* ES4326 expressing a*vrB* at an OD_{600} = 0.2 in 10 mM $MgCl_2$ to induce SAR or 10 mM $MgCl_2$ without bacteria (mock). 24 hours after inoculation, the upper uninoculated leaves were challenged with *P.s.m.* ES4326 at OD_{600} = 0.001. Leaf discs within the infiltrated systemic area were taken immediately (Day 0) and 3 days after inoculation (Day 3) to measure the bacterial growth in those leaves.

Cellular distribution of snc1-GFP

0.5 g of three-week-old plants were harvested and ground to a fine powder in liquid nitrogen and mixed with 2 volumes of lysis buffer (20 mM Tris-HCl, pH 7.4, 25% glycerol, 20 mM KCl, 2 mM EDTA, 2.5 mM $MgCl_2$, 250 mM sucrose and 1 mM PMSF). The homogenate was filtered through a 95 and 37 μm nylon netting successively. The flow-through was spun at 1500 *g* for 10 minutes and the supernatant consisting of the cytosolic fraction was collected and mixed with 5x Laemmli loading buffer and heated at 95˚C for 5 minutes. The pellet was washed 4 times with 5 mL of nuclear resuspension buffer NRBT consisting of 20 mM Tris-HCl, pH 7.4, 25% glycerol, 2.5 mM $MgCl_2$ and 0.2% Triton X-100. The final pellet was mixed with 50 μL of 1x Laemli buffer and heated at 95˚C for 5 minutes. 50 μL of each fraction was loaded on an 8 % SDS-PAGE gel for protein seperation. Antibodies used for immunoblot analyses were as described: anti-Histone H3 (Feys et al., 2005), anti-GFP (Wirthmueller et al., 2007) and anti-PEPC (Noël et al., 2007). Band intensities were measured by Quantity One 4.6.1 software (BioRad).

NPR1 and EDS1 protein expression and localization analyses

For NPR1 protein extraction from INA-induced tissues, 4-week-old plants were sprayed to imminent runoff with an aqueous solution of 0.65 mM 2,6-dichloroisonicotinic acid (INA) with 0.01 % Silwett L-77 surfactant. Plants were harvested 24 h after being sprayed for the first time and 3 h after being treated a second time with INA. Total protein extracts and preparation of nuclear/nuclei-depleted protein extracts were described previously (Feys et al., 2005). Anti-EDS1 antibody used for Western blot analysis was described earlier (Feys et al., 2005).

Acknowledgements

We thank the ABRC for seeds of *mos7-2* and *mos7-3* and Dr. Roger Innes for *P.s.t.* DC3000 carrying *avrPphB*. We also appreciate Drs. Fred Sack and EunKyoung Lee for their help with confocal microscopy. The research is supported by funds to XL from the Natural Sciences and Engineering Research Council of Canada (NSERC), the Canadian Foundation for Innovation (CFI), the British Columbia Knowledge Development Fund (BCKDF), the UBC Blusson Fund and the UBC Michael Smith Laboratories. We are thankful for a Feodor Lynen research fellowship of the Alexander von Humboldt Foundation to MW, and a Le Fonds québécois de la recherche sur la nature et les technologies to HG. JEP is grateful for an IMPRS PhD fellowship supporting AVG and Deutsche Forschungsgemeinschaft 'SFB 670' funding of LW.

References

Aarts N., Metz M., Holub E., Staskawicz B.J., Daniels M.J., and Parker J.E. (1998). Different requirements for *EDS1* and *NDR1* by disease resistance genes define at least two *R* gene-mediated signaling pathways in *Arabidopsis*. Proc. Natl. Acad. Sci. USA **95,** 10306-11.

Axtell M.J. and Staskawicz B.J. (2003). Initiation of *RPS2*-specified disease resistance in *Arabidopsis* is coupled to the AvrRpt2-directed elimination of RIN4. Cell **112,** 369-77.

Belkhadir Y., Subramaniam R., and Dangl J.L. (2004). Plant disease resistance protein signaling: NBS-LRR proteins and their partners. Curr. Opin. Plant Biol. **7,** 391-399.

Bernad R., van der Velde H., Fornerod M., and Pickersgill H. (2004). Nup358/RanBP2 attaches to the nuclear pore complex via association with Nup88 and Nup214/CAN and plays a supporting role in CRM1-mediated nuclear protein export. Mol. Cell. Biol. **24,** 2373-2384.

Burch-Smith T.M., Schiff M., Caplan J.L., Tsao J., Czymmek K., and Dinesh-Kumar S.P. (2007). A Novel Role for the TIR Domain in Association with Pathogen-Derived Elicitors. PLoS Biol. **5,** e68.

Cao H., Bowling S.A., Gordon A.S., and Dong X. (1994). Characterization of an Arabidopsis Mutant That Is Nonresponsive to Inducers of Systemic Acquired-Resistance. Plant Cell **6,** 1583-1592.

Cao H., Glazebrook J., Clarke J.D., Volko S., and Dong X. (1997). The Arabidopsis *NPR1* gene that controls systemic acquired resistance encodes a novel protein containing ankyrin repeats. Cell **88,** 57-63.

Century K.S., Shapiro A.D., Repetti P.P., Dahlbeck D., Holub E., and Staskawicz B.J. (1997). *NDR1*, a pathogen-induced component required for *Arabidopsis* disease resistance. Science **278,** 1963-1965.

Clough S.J. and Bent A.F. (1998). Floral dip: a simplified method for *Agrobacterium*-mediated transformation of *Arabidopsis thaliana*. Plant J. **16,** 735-743.

Coppinger P., Repetti P.P., Day B., Dahlbeck D., Mehlert A., and Staskawicz B.J. (2004). Overexpression of the plasma membrane-localized NDR1 protein results in enhanced bacterial disease resistance in *Arabidopsis thaliana*. Plant J. **40,** 225-237.

Dockendorff T.C., Heath C.V., Goldstein A.L., Snay C.A., and Cole C.N. (1997). C-terminal truncations of the yeast nucleoporin Nup145p produce a rapid temperature-conditional mRNA export defect and alterations to nuclear structure. Mol. Cell. Biol. **17,** 906-920.

Dong C.H., Hu X., Tang W., Zheng X., Kim Y.S., Lee B.H., and Zhu J.K. (2006). A putative *Arabidopsis* nucleoporin, AtNUP160, is critical for RNA export and required for plant tolerance to cold stress. Mol. Cell. Biol. **26,** 9533-9543.

Durrant W.E. and Dong X. (2004). Systemic acquired resistance. Annu Rev Phytopathol **42,** 185-209.

Emtage J.L., Bucci M., Watkins J.L., and Wente S.R. (1997). Defining the essential functional regions of the nucleoporin Nup145p. J. Cell. Sci. **110 (Pt 7),** 911-925.

Faria A.M., Levay A., Wang Y., Kamphorst A.O., Rosa M.L., Nussenzveig D.R., Balkan W., Chook Y.M., Levy D.E., and Fontoura B.M. (2006). The nucleoporin Nup96 is required for proper expression of interferon-regulated proteins and functions. Immunity **24,** 295-304.

Feys B.J., Moisan L.J., Newman M.A., and Parker J.E. (2001). Direct interaction between the *Arabidopsis* disease resistance signaling proteins, EDS1 and PAD4. Embo J. **20,** 5400-5411.

Feys B.J., Wiermer M., Bhat R.A., Moisan L.J., Medina-Escobar N., Neu C., Cabral A., and Parker J.E. (2005). *Arabidopsis* SENESCENCE-ASSOCIATED GENE101 stabilizes and signals within an ENHANCED DISEASE SUSCEPTIBILITY1 complex in plant innate immunity. Plant Cell **17,** 2601-2613.

Grant M.R., Godiard L., Straube E., Ashfield T., Lewald J., Sattler A., Innes R.W., and Dangl J.L. (1995). Structure of the *Arabidopsis RPM1* gene enabling dual specificity disease resistance. Science **269,** 843-6.

Haasen D., Kohler C., Neuhaus G., and Merkle T. (1999). Nuclear export of proteins in plants: AtXPO1 is the export receptor for leucine-rich nuclear export signals in *Arabidopsis thaliana*. Plant J. **20,** 695-705.

Haseloff J., Siemering K.R., Prasher D.C., and Hodge S. (1997). Removal of a cryptic intron and subcellular localization of green fluorescent protein are required to mark transgenic *Arabidopsis* plants brightly. Proc. Natl. Acad. Sci. USA **94,** 2122-2127.

Hellens R.P., Edwards E.A., Leyland N.R., Bean S., and Mullineaux P.M. (2000). pGreen: a versatile and flexible binary Ti vector for *Agrobacterium*-mediated plant transformation. Plant Mol. Biol. **42,** 819-832.

Hinsch M. and Staskawicz B. (1996). Identification of a new *Arabidopsis* disease resistance locus, *RPS4*, and cloning of the corresponding avirulence gene, *avrRps4*, from *Pseudomonas syringae* pv. *pisi*. Mol. Plant Microbe Interact. **9,** 55-61.

Jander G., Norris S.R., Rounsley S.D., Bush D.F., Levin I.M., and Last R.L. (2002). Arabidopsis map-based cloning in the post-genome era. Plant Physiol. **129,** 440-450.

Jones J.D. and Dangl J.L. (2006). The plant immune system. Nature **444,** 323-9.

Kim M.G., da Cunha L., McFall A.J., Belkhadir Y., DebRoy S., Dangl J.L., and Mackey D. (2005). Two *Pseudomonas syringae* type III effectors inhibit RIN4-regulated basal defense in *Arabidopsis*. Cell **121,** 749-59.

Li X., Zhang Y., Clarke J.D., Li Y., and Dong X. (1999). Identification and cloning of a negative regulator of systemic acquired resistance, SNlI1, through a screen for suppressors of *npr1-1*. Cell **98,** 329-339.

Li X., Clarke J.D., Zhang Y., and Dong X. (2001). Activation of an EDS1-mediated R-gene pathway in the *snc1* mutant leads to constitutive, NPR1-independent pathogen resistance. Mol. Plant Microbe Interac. **14,** 1131-1139.

Mackey D., Holt B.F., Wiig A., and Dangl J.L. (2002). RIN4 interacts with *Pseudomonas syringae* type III effector molecules and is required for RPM1-mediated resistance in *Arabidopsis*. Cell **108,** 743-54.

Mackey D., Belkhadir Y., Alonso J.M., Ecker J.R., and Dangl J.L. (2003). *Arabidopsis* RIN4 is a target of the type III virulence effector AvrRpt2 and modulates RPS2-mediated resistance. Cell **112,** 379-389.

Martin G.B., Bogdanove A.J., and Sessa G. (2003). Understanding the functions of plant disease resistance proteins. Annu. Rev. Plant. Biol. **54,** 23-61.

McHale L., Tan X., Koehl P., and Michelmore R.W. (2006). Plant NBS-LRR proteins: adaptable guards. Genome Biol. **7,** 212.

Mou Z., Fan W.H., and Dong X. (2003). Inducers of plant systemic acquired resistance regulate NPR1 function through redox changes. Cell **113,** 935-944.

Noel L.D., Cagna G., Stuttmann J., Wirthmuller L., Betsuyaku S., Witte C.P., Bhat R., Pochon N., Colby T., and Parker J.E. (2007). Interaction between SGT1 and cytosolic/nuclear HSC70 chaperones regulates *Arabidopsis* immune responses. Plant Cell **19,** 4061-4076.

Palma K., Zhang Y., and Li X. (2005). An importin α homolog, MOS6, plays an important role in plant innate immunity. Curr. Biol. **15,** 1129-35.

Palma K., Zhao Q., Cheng Y.T., Bi D., Monaghan J., Cheng W., Zhang Y., and Li X. (2007). Regulation of plant innate immunity by three proteins in a complex conserved across the plant and animal kingdoms. Genes Dev. **21,** 1484-1493.

Parry G., Ward S., Cernac A., Dharmasiri S., and Estelle M. (2006). The *Arabidopsis* SUPPRESSOR OF AUXIN RESISTANCE proteins are nucleoporins with an important role in hormone signaling and development. Plant Cell **18,** 1590-1603.

Roth P., Xylourgidis N., Sabri N., Uv A., Fornerod M., and Samakovlis C. (2003). The *Drosophila* nucleoporin DNup88 localizes DNup214 and CRM1 on the nuclear envelope and attenuates NES-mediated nuclear export. J. Cell Biol. **163,** 701-706.

Sacco M.A., Mansoor S., and Moffett P. (2007). A RanGAP protein physically interacts with the NB-LRR protein Rx, and is required for Rx-mediated viral resistance. Plant J. **52,** 82-93.

Shah J. (2003). The salicylic acid loop in plant defense. Curr. Opin. Plant Biol. **6,** 365-371.

Shen Q.H., Saijo Y., Mauch S., Biskup C., Bieri S., Keller B., Seki H., Ülker B., Somssich I.E., and Schulze-Lefert P. (2007). Nuclear activity of MLA immune receptors links isolate-specific and basal disease-resistance responses. Science **315,** 1098-1103.

Simonich M.T. and Innes R.W. (1995). A disease resistance gene in Arabidopsis with specificity for the avrPph3 gene of *Pseudomonas syringae* pv. *phaseolicola*. Mol. Plant Microbe Interact. **8,** 637-640.

Tada Y., Spoel S.H., Pajerowska-Mukhtar K., Mou Z., Song J., and Dong X. (2008). Plant Immunity Requires Conformational Changes of NPR1 via S-Nitrosylation and Thioredoxins. Science **321**, 952-956.

Takahashi N., van Kilsdonk J.W., Ostendorf B., Smeets R., Bruggeman S.W., Alonso A., van de Loo F., Schneider M., van den Berg W.B., and Swart G.W. (2008). Tumor marker nucleoporin 88 kDa regulates nucleocytoplasmic transport of NF-κB. Biochem. Biophys. Res. Commun. **374**, 424-430.

Tameling W.I. and Baulcombe D.C. (2007). Physical Association of the NB-LRR Resistance Protein Rx with a Ran GTPase-Activating Protein Is Required for Extreme Resistance to *Potato virus X*. Plant Cell **19,** 1682-1694.

Terry L.J., Shows E.B., and Wente S.R. (2007). Crossing the nuclear envelope: hierarchical regulation of nucleocytoplasmic transport. Science **318,** 1412-1416.

Uv A.E., Roth P., Xylourgidis N., Wickberg A., Cantera R., and Samakovlis C. (2000). *members only* encodes a *Drosophila* nucleoporin required for Rel protein import and immune response activation. Genes Dev. **14,** 1945-57.

van der Biezen E.A., Freddie C.T., Kahn K., Parker J.E., and Jones J.D. (2002). *Arabidopsis RPP4* is a member of the *RPP5* multigene family of TIR-NB-LRR genes and confers downy mildew resistance through multiple signalling components. Plant J. **29,** 439-51.

Vernooij B., Friedrich L., Morse A., Reist R., Kolditz-Jawhar R., Ward E., Uknes S., Kessmann H., and Ryals J. (1994). Salicylic Acid Is Not the Translocated Signal Responsible for Inducing Systemic Acquired Resistance but Is Required in Signal Transduction. Plant Cell **6,** 959-965.

Wiermer M., Feys B.J., and Parker J.E. (2005). Plant immunity: the EDS1 regulatory node. Curr. Opin. Plant Biol. **8,** 383-389.

Wirthmueller L., Zhang Y., Jones J.D., and Parker J.E. (2007). Nuclear accumulation of the *Arabidopsis* immune receptor RPS4 is necessary for triggering EDS1-dependent defense. Curr. Biol. **17,** 2023-2029.

Xylourgidis N., Roth P., Sabri N., Tsarouhas V., and Samakovlis C. (2006). The nucleoporin Nup214 sequesters CRM1 at the nuclear rim and modulates NFκB activation in *Drosophila*. J. Cell. Sci. **119,** 4409-4419.

Zhang Y., Fan W., Kinkema M., Li X., and Dong X. (1999). Interaction of NPR1 with basic leucine zipper protein transcription factors that bind sequences required for salicylic acid induction of the *PR-1* gene. Proc. Natl. Acad. Sci. USA **96,** 6523-8.

Zhang Y., Goritschnig S., Dong X., and Li X. (2003a). A gain-of-function mutation in a plant disease resistance gene leads to constitutive activation of downstream signal transduction pathways in *suppressor of npr1-1*, *constitutive 1*. Plant Cell **15,** 2636-2646.

Zhang Y., Tessaro M.J., Lassner M., and Li X. (2003b). Knockout analysis of Arabidopsis transcription factors *TGA2*, *TGA5*, and *TGA6* reveals their redundant and essential roles in systemic acquired resistance. Plant Cell **15,** 2647-2653.

Zhang Y. and Li X. (2005). A Putative Nucleoporin 96 Is Required for Both Basal Defense and Constitutive Resistance Responses Mediated by *suppressor of npr1-1*, *constitutive 1*. Plant Cell **17,** 1306-1316.

Supplementary Table 1. Molecular markers used for map-based cloning of *mos7-1*.

BAC Name	Primer Name	Primer Sequence (5'→3')	Polymorphism (Col-0/Ler)
K18I23	K18I23-F	AGATTCCAGCTCCGACGATG	172bp/205bp
	K18I23-R	ACGCGCCAAAAGTGCGTGTC	
MOP10	MOP10-F	CTACATGTCCATAGAACCTTC	118bp/129bp
	MOP10-R	CAGTTCTATCATGTATCCACC	
MJJ3	MJJ3-3F	TCTGACTCAATATGAGAGTCC	117bp/108bp
	MJJ3-3R	ATAACTTTATGGGCTGCAGTG	
K18J17	K18J17-F	CGCGATTAAAGATCCGGTA	119bp/107bp
	K18J17-R	TCGAGCAATAAGAGTGATTCC	
MHF15	MHF15-F	CAGAAAGGTCATGAAACCTAG	212bp/159bp
	MHF15-R	GAGCACCAATAAGGTTTCCTC	

Cheng_Fig1

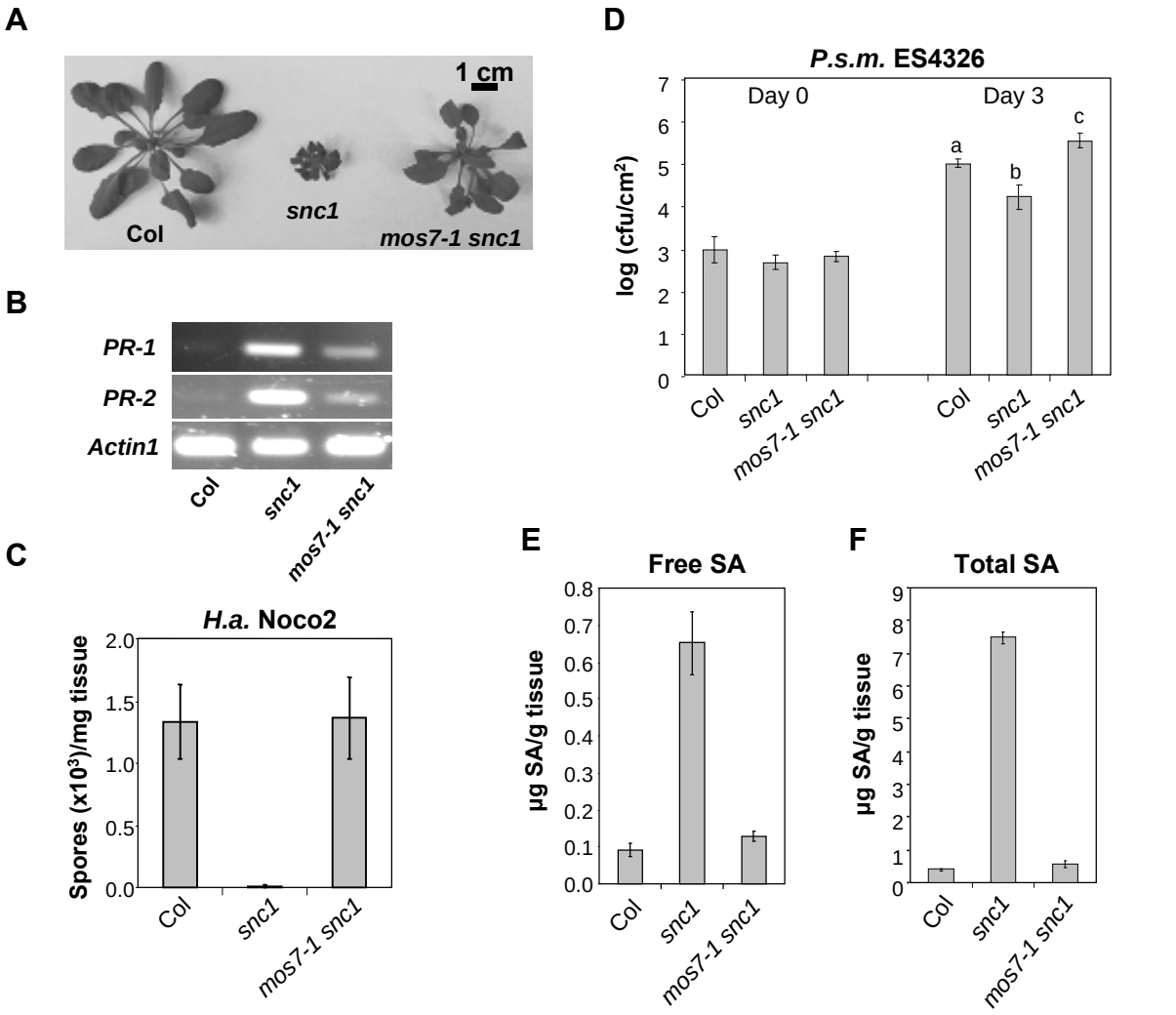

Figure 1. *mos7-1* suppresses the autoimmune responses in *snc1*.
(A) Morphology of five-week-old soil-grown plants of Col, *snc1*, and *mos7-1 snc1*.
(B) *PR* gene expression in *mos7-1 snc1*. RNAs were prepared from three-week-old plants grown on MS media and reverse transcribed to obtain total cDNA. The cDNA samples were normalized by real-time PCR using *Actin1*. *PR-1*, *PR-2*, and *Actin1* were amplified by 31 cycles of PCR using equal amounts of total cDNA, and the products were analyzed by agarose gel electrophoresis with ethidium bromide staining.
(C) Two-week-old soil-grown seedlings were inoculated with *H.a.* Noco2 at a concentration of 50,000 conidia per ml of water and the number of conidia was quantified 7 days post inoculation (dpi). Bars represent means of four replicates ± standard deviation (SD).
(D) Five-week-old soil-grown plants were infiltrated with *P.s.m.* ES4326 (OD_{600}=0.0001) and colony forming units (cfu) were quantified at 0 and 3 dpi, respectively. Bars represent means of six replicates ± SD. All data were analyzed by one-way analysis of variance (oneway ANOVA). Different letters indicate statistically significant differences between genotypes ($P<0.05$).
(E) Free and (F) total SA were extracted from five-week-old plants and analyzed by HPLC. Bars represent the average of four replicates ± SD.

Cheng_Fig2

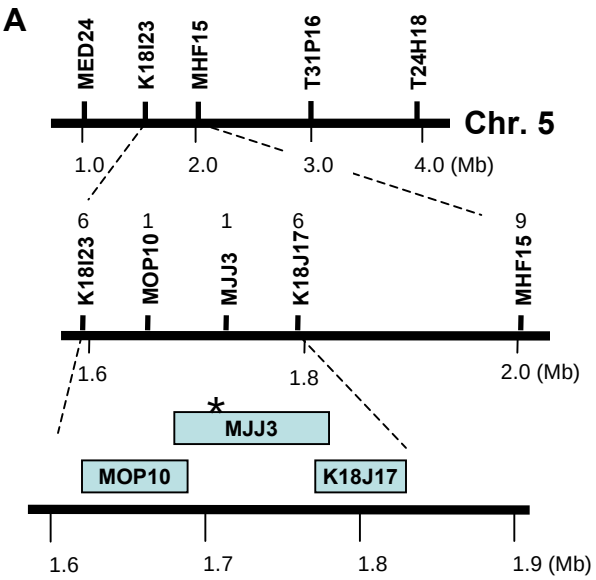

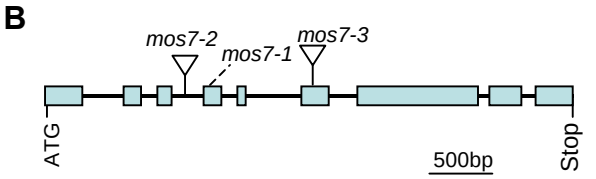

C

```
MOS7     gtatgctAGGCTTTTCGATTTGTCTTCAGATACTGAGC
         ||||||||||||           ||||||||||||||||
mos7-1   gtatgctAGGCT------------TTCAGATACTGAGC
```

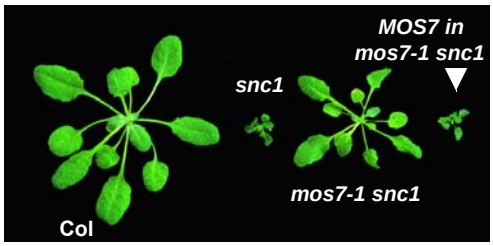

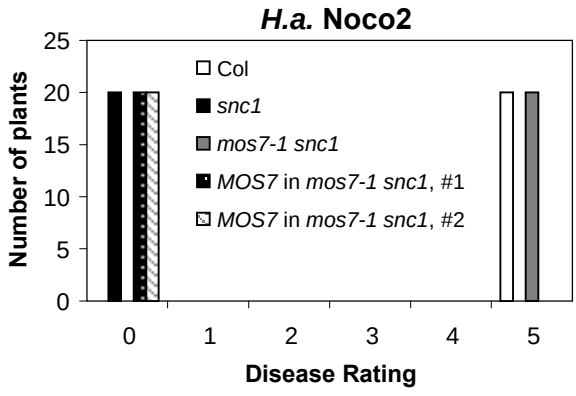

Figure 2. Map-based cloning of *mos7-1*.
(A) Map position of the *mos7-1* locus on chromosome 5. BAC clones and number of recombinants are indicated. Asterisk indicates the physical location of the *mos7-1* locus.
(B) Gene structure of *At5g05680*. The exons are indicated by boxes, and the introns are represented by solid lines. Locations of *mos7-1* deletion and T-DNA insertions of *mos7-2* (SALK_129301) and *mos7-3* (SALK_085349) are indicated.
(C) *mos7-1* deletion at the DNA level. Lower and upper case letters indicate intron and exon, respectively.
(D) Morphology of wild type Col, *snc1*, *mos7-1 snc1*, and a representing transgenic line containing *MOS7* transgene driven by its native promoter in *snc1 mos7-1*.
(E) Resistance of Col, *snc1*, *mos7-1 snc1*, and a *MOS7* complementing line in *snc1 mos7-1* against *H.a.* Noco2. The infection was rated as follows on 20 plants 7 days after infection by counting the number of conidiophores per infected leaf: 0, no conidiophores on the plants; 1, no more than 5 conidiophores per infected leaf; 2, 6 to 20 conidiophores on a few of the infected leaves; 3, 6 to 20 conidiophores on most of the infected leaves; 4, 5 or more conidiophores on all infected leaves; 5, 20 or more conidiophores on all infected leaves.

Cheng_Fig3

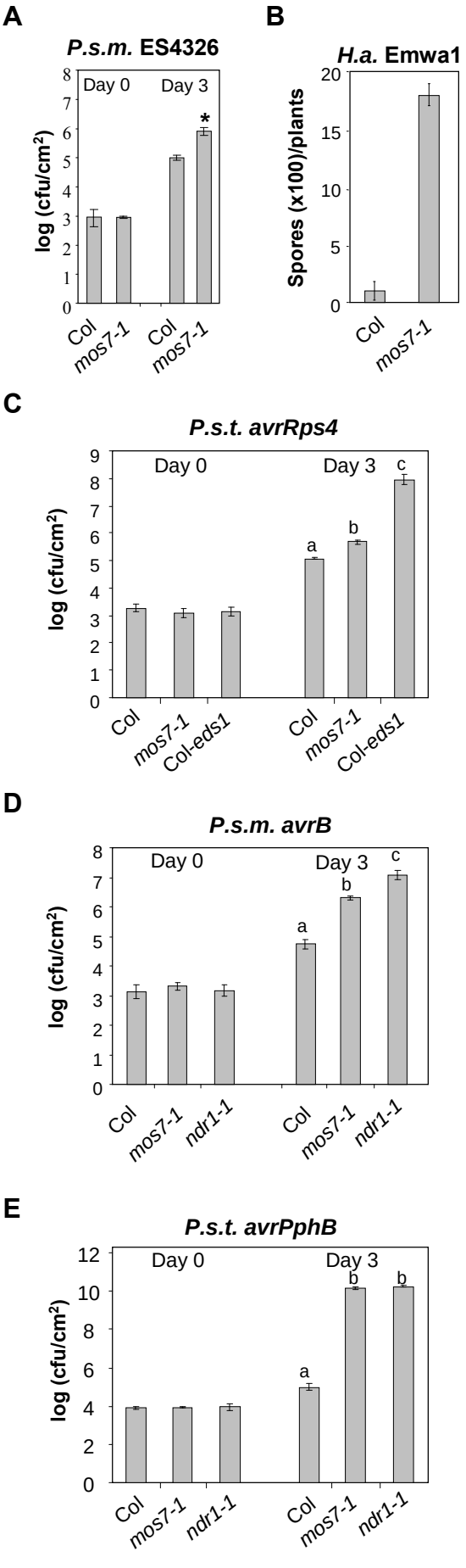
A
P.s.m. ES4326
Day 0
Day 3
log (cfu/cm²)
*
Col
mos7-1
Col
mos7-1
B
H.a. Emwa1
Spores (x100)/plants
Col
mos7-1
C
P.s.t. avrRps4
Day 0
Day 3
log (cfu/cm²)
a
b
c
Col
mos7-1
Col-eds1
Col
mos7-1
Col-eds1
D
P.s.m. avrB
Day 0
Day 3
log (cfu/cm²)
a
b
c
Col
mos7-1
ndr1-1
Col
mos7-1
ndr1-1
E
P.s.t. avrPphB
Day 0
Day 3
log (cfu/cm²)
a
b
b
Col
mos7-1
ndr1-1
Col
mos7-1
ndr1-1

Figure 3. Altered basal and R-protein mediated resistance in *mos7-1* single mutant plants.

(A) Enhanced disease susceptibility to *P.s.m*. ES4326 in *mos7-1*. The plants were infiltrated with the bacteria at OD_{600} = 0.0001. Leaf discs within the infiltrated area were taken at Day 0 and Day 3 to measure the bacterial growth. Bars represent means of six replicates ± SD. Susceptibility toward *P.s.m.* ES4326 in *mos7-1* is significantly enhanced compared to Col as indicated by the asterisk ($p<0.0001$, t test).

(B to E) *mos7-1* mutant plants were challenged with the indicated avirulent pathogens carrying effectors that can trigger the cognate R protein-mediated resistance. (B) 50,000 conidia/ml was used for *H.a.* Emwa1 inoculation. (C-E) For bacterial pathogens, an inoculation dose of OD600 = 0.002 was used. Bars represent means of six replicates ± SD. Statistical analyses of the bacterial growth assays in C, D, and E were done by using one-way ANOVA provided by StatsDirect statistical software (StatsDirect Ltd. http://www.statsdirect.com. England: StatsDirect Ltd. 2008). Statistical differences among the samples are labelled with different letters ($P<0.05$).

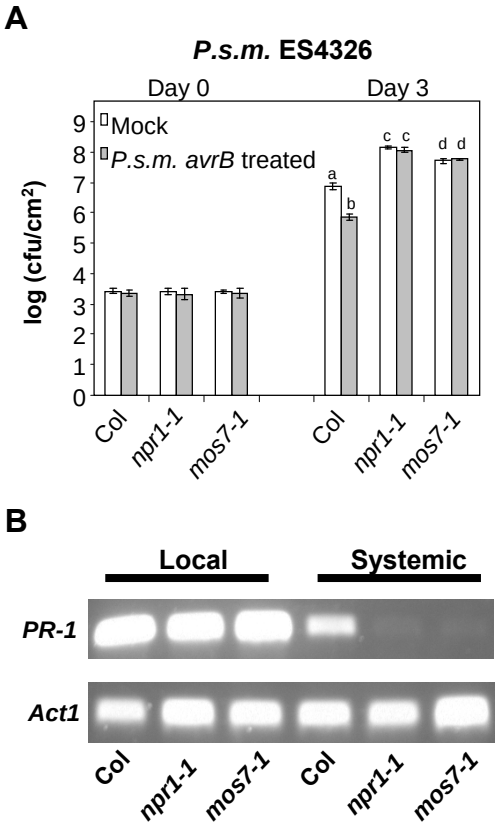

Figure 4. Systemic acquired resistance is compromised in *mos7-1*.
(A) Growth of *P.s.m.* ES4326 in five-week-old Col, *npr1-1* and *mos7-1* plants pre-inoculated with *P.s.m.* ES4326 *avrB* in 10 mM $MgCl_2$ (grey bars) or 10mM $MgCl_2$ alone (mock; white bars). Bars represent means of four replicates ± SD. Different letters indicate statistically significant differences between genotypes ($P<0.05$).
(B) Semi-quantitative RT-PCR for *PR-1* on RNA extracted from local and systemic leaves of the indicated genotypes pre-treated with *P.s.m.* ES4326 *avrB*. *Actin1* was used as control.

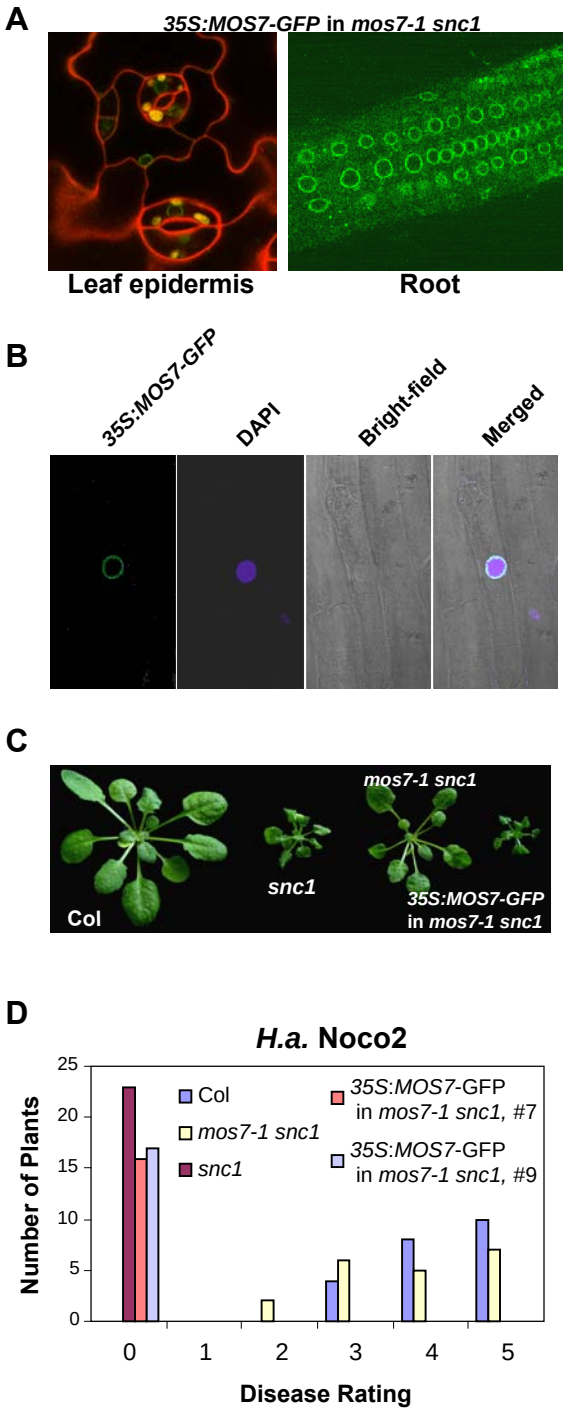

Figure 5. Subcellular localization of MOS7-GFP.

(A) MOS7-GFP fluorescence in leaf pavement and root cells of *mos7-1 snc1* transgenic plants expressing *MOS7-GFP* under the control of *35S* promoter. Plant cell walls were stained with 5mg/ml propidium iodine (red).

(B) MOS7-GFP fluorescence, DAPI staining of the nucleus, bright-field, and merged fluorescence channels in root cells.

(C) Complementation of *mos7-1* by *MOS7-GFP* expressed by the *35S* promoter.

(D) Restoration of enhanced disease resistance in *mos7-1 snc1* transformed with *MOS7-GFP* driven by *35S* promoter. The disease ratings are as described in Figure 2E.

Cheng_Fig6

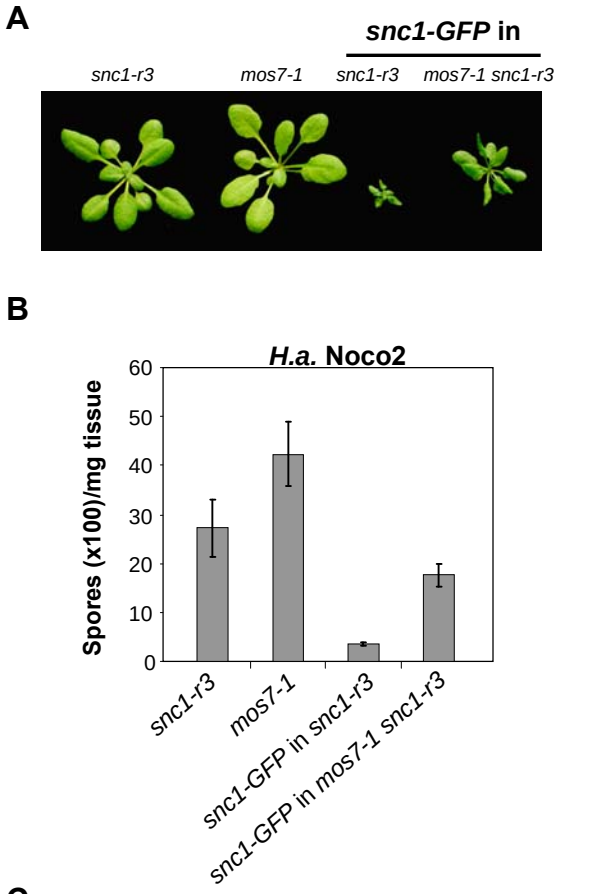
A
snc1-GFP in
snc1-r3
mos7-1
snc1-r3
mos7-1 snc1-r3
B
H.a. Noco2
Spores (x100)/mg tissue
60
50
40
30
20
10
0
snc1-r3
mos7-1
snc1-GFP in snc1-r3
snc1-GFP in mos7-1 snc1-r3
C
snc1-GFP in
kDa
snc1-r3
mos7-1
snc1-r3
mos7-1 snc1-r3
250
150
100
α-GFP
α-PEPC
D
snc1-GFP in
snc1-r3
mos7-1
snc1-r3
mos7-1 snc1-r3
kDa
ΔN
N
ΔN
N
ΔN
N
ΔN
N
250
150
100
20
15
α-GFP
α-PEPC
α-Histone H3

Figure 6. Abundance and cellular distribution of snc1-GFP in *mos7-1 snc1-r3.*
(A) Morphology of three-week-old plants of *snc1-r3*, *mos7-1*, *snc1-GFP* in *snc1-r3*, and *snc1-GFP* in *mos7-1 snc1-r3*.
(B) *H.a.* Noco2 growth on the same genotypes as (A).
(C) Immunoblot analysis of snc1-GFP expressed under its native promoter in total protein extracts of unchallenged leaf tissues in *snc1-r3* and *mos7-1 snc1-r3*. Equal loading was monitored by probing the membrane with anti-PEPC.
(D) Immunoblot analysis of snc1-GFP in nuclei-depleted (ΔN) and nuclear (N) protein extracts of the indicated genotypes. Anti-PEPC was used as a cytosolic marker and anti-Histone H3 was used as a nuclear marker. Nuclear protein extracts (N) were 20x concentrated as compared to nuclei-depleted fractions (ΔN)

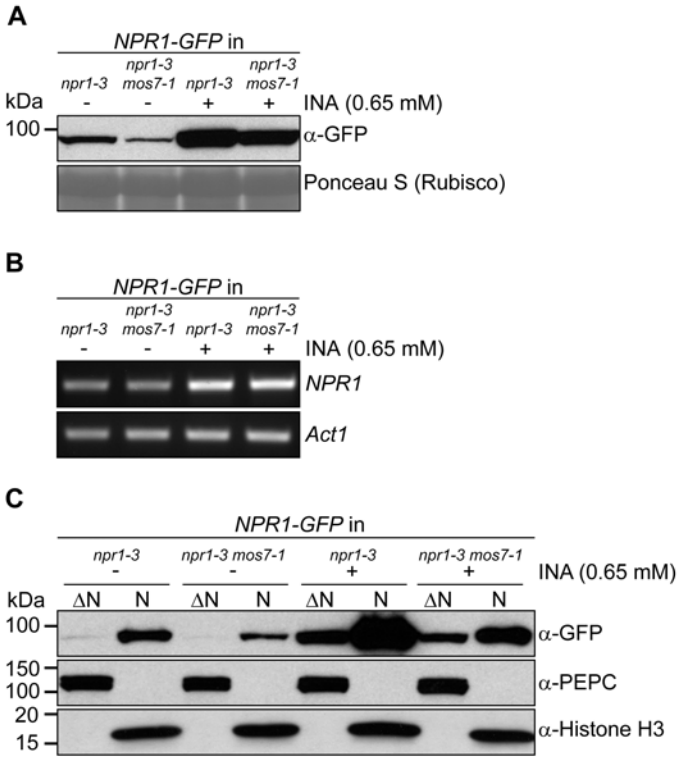

Figure 7. NPR1 protein abundance and subcellular localization in *mos7-1*.
(A) NPR1-GFP expressed by its native promoter in *mos7-1*. Immunoblot analysis of NPR1-GFP in total protein extracts of unchallenged leaf tissues (-) and leaf tissues harvested 24 h after spraying plants with 0.65 mM INA (+). Equal loading was monitored by staining the membrane with Ponceau S.
(B) Semiquantitative RT-PCR for *NPR1* on RNA extracted from 4-week old plants of the indicated genotypes treated with or without INA. *Actin1* expression was used as control.
(C) Immunoblot analysis of NPR1-GFP in nuclei-depleted (ΔN) and nuclear (N) protein extracts of unchallenged (-) and INA treated (+) tissues of the indicated genotypes. Anti-PEPC was used as a cytosolic marker and anti-Histone H3 was used as a nuclear marker. Nuclear protein extracts (N) were 35x concentrated as compared to nuclei-depleted fractions (ΔN).

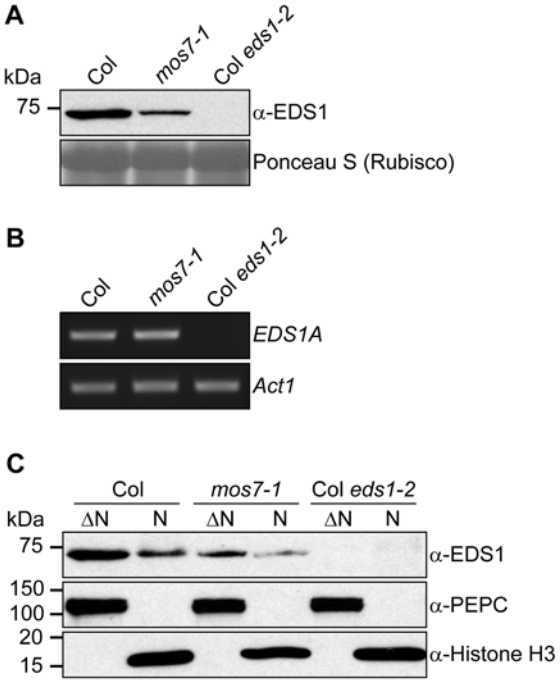

Figure 8. EDS1 protein abundance and subcellular localization in *mos7-1*.
(A) EDS1 in *mos7-1*. Immunoblot analysis of EDS1 in total protein extracts of unchallenged leaf tissues. Equal loading was monitored by staining the membrane with Ponceau S.
(B) Semiquantitative RT-PCR for *EDS1A* on RNA extracted from 4-week old unchallenged plants of the indicated genotypes. *Actin1* expression was used as control.
(C) Immunoblot analysis of EDS1 in nuclei-depleted (ΔN) and nuclear (N) protein extracts of unchallenged leaf tissues. Anti-PEPC was used as a cytosolic marker and anti-Histone H3 was used as a nuclear marker. Nuclear protein extracts (N) were 35x concentrated as compared to nuclei-depleted fractions (ΔN).

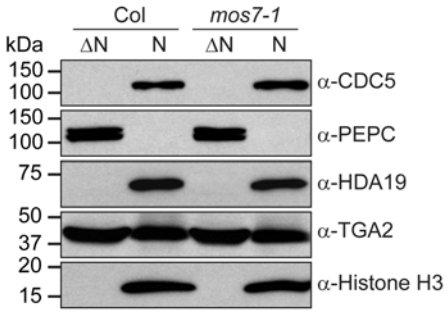

Figure 9. CDC5, PEPC, HDA19, TGA2 and Histone H3 protein abundance and subcellular localization is unaltered in *mos7-1*.
Immunoblot analysis of CDC5, PEPC, HDA19, TGA2 and Histone H3 in nuclei-depleted (ΔN) and nuclear (N) protein extracts of unchallenged leaf tissues. Nuclear protein extracts (N) were 35x concentrated as compared to nuclei-depleted fractions (ΔN).

Cheng_Sup Fig1

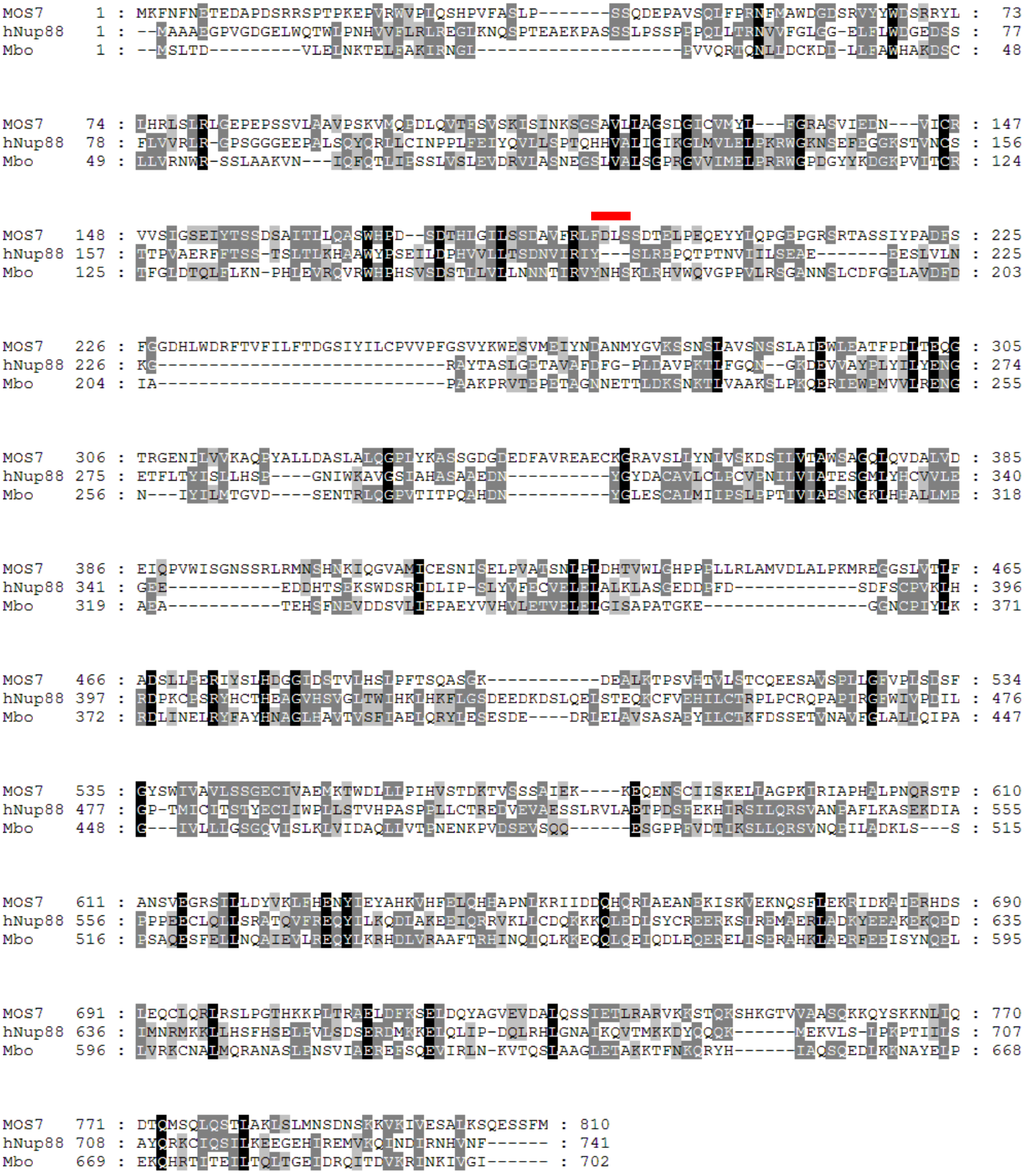

Supplementary Figure 1. Amino acid alignment of MOS7, human Nup88, and *Drosophila* Nup88.
Amino acid sequences from *Arabidopsis* MOS7 (accession number NP_196187), *Drosophila* DNup88 (Mbo; accession number NP_524330), and human hNup88 (accession number NP_002523) were aligned using ClustalW2 (Larkin et al. 2007). Sequence identities and similarities were shaded using Genedoc. Red bar indicates the 4 amino acids deleted in mos7-1. Identical amino acids are shaded in black, and amino acids with similar properties are shaded in grey.

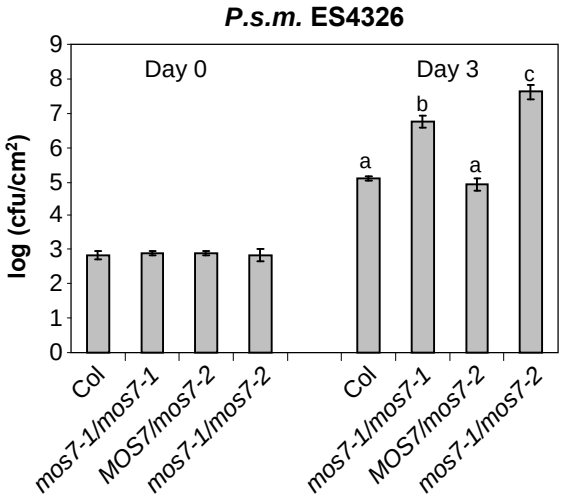

Supplementary Figure 2. Allelism test between *mos7-1* and *mos7-2* using *P.s.m.* ES4326.

F1 plants from *mos7-1* × *mos7-2* that carry one copy of each mutation were challenged with *P.s.m*. ES4326 at OD_{600} = 0.0001. Leaf discs within the infiltrated area were taken at Day 0 and Day 3 to measure the bacterial growth in the leaves. Data were analyzed by one-way ANOVA. Different letters indicate statistically significant differences between genotypes. The bars represent averages of four replicates ± SD.

Cheng_Sup Fig3

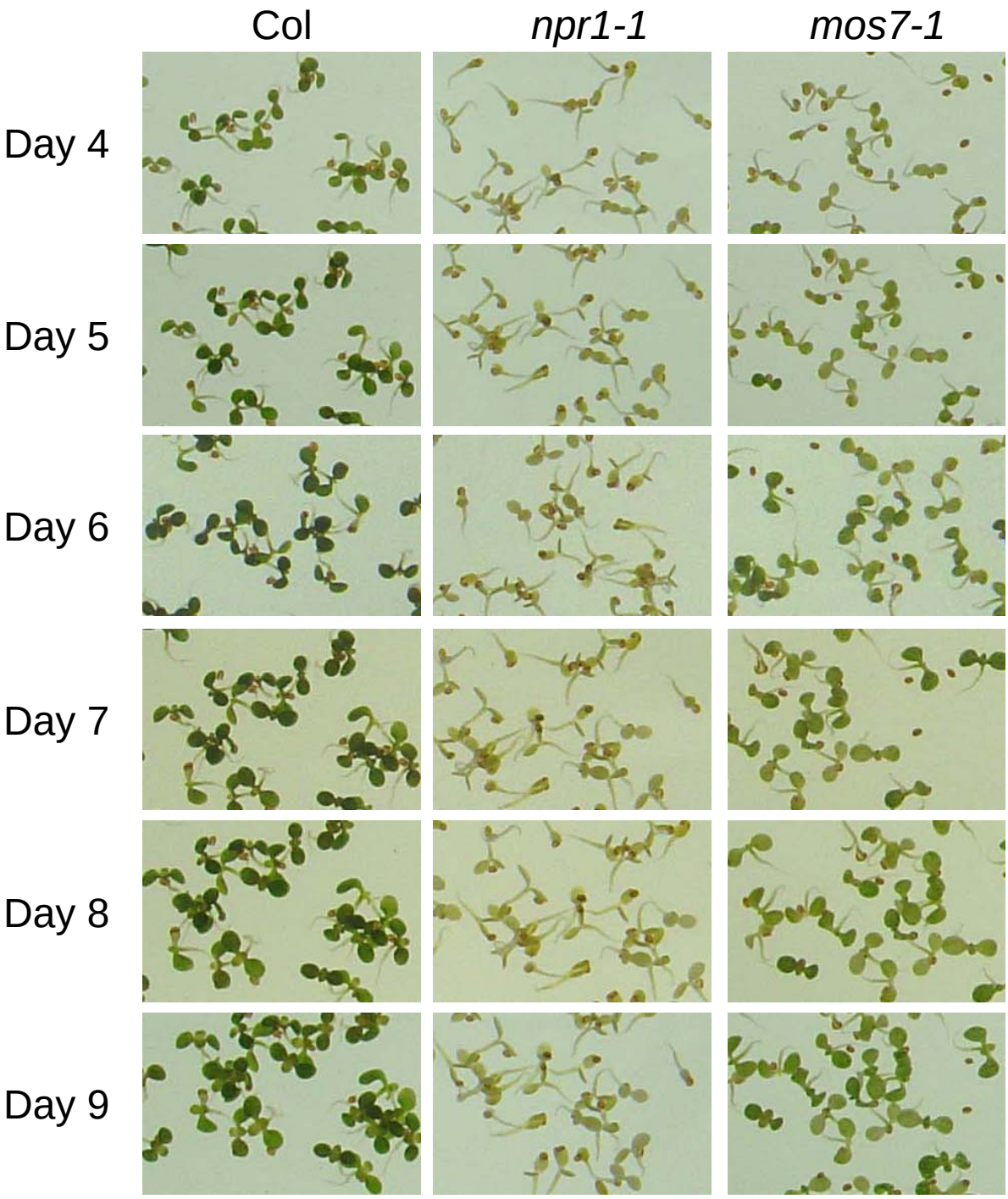

Supplementary Figure 3. Tolerance of Col, *npr1-1*, and *mos7-1* plants to high concentrations of SA. Seeds were plated on MS medium containing 0.2 mM SA, and the pictures were taken from 4 to 9 days after germination.

Cheng_Sup Fig4

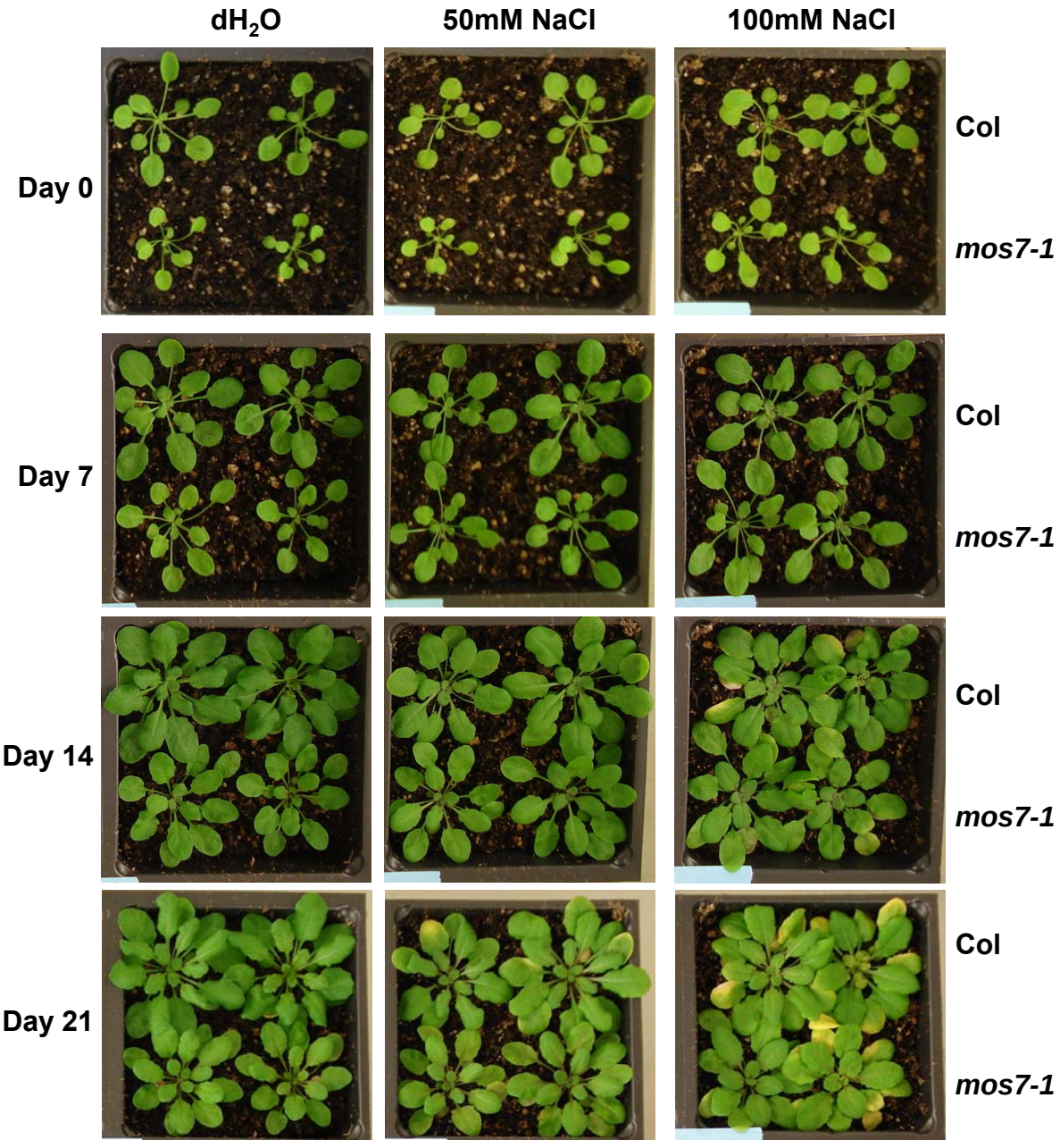

Supplementary Figure 4. Tolerance of Col and *mos7-1* plants to high concentrations of sodium chloride. Plants with 8 to 10 rosette leaves were flooded every 3 days with either distilled water (dH_2O; Control), 50mM, or 100 mM NaCl solution.

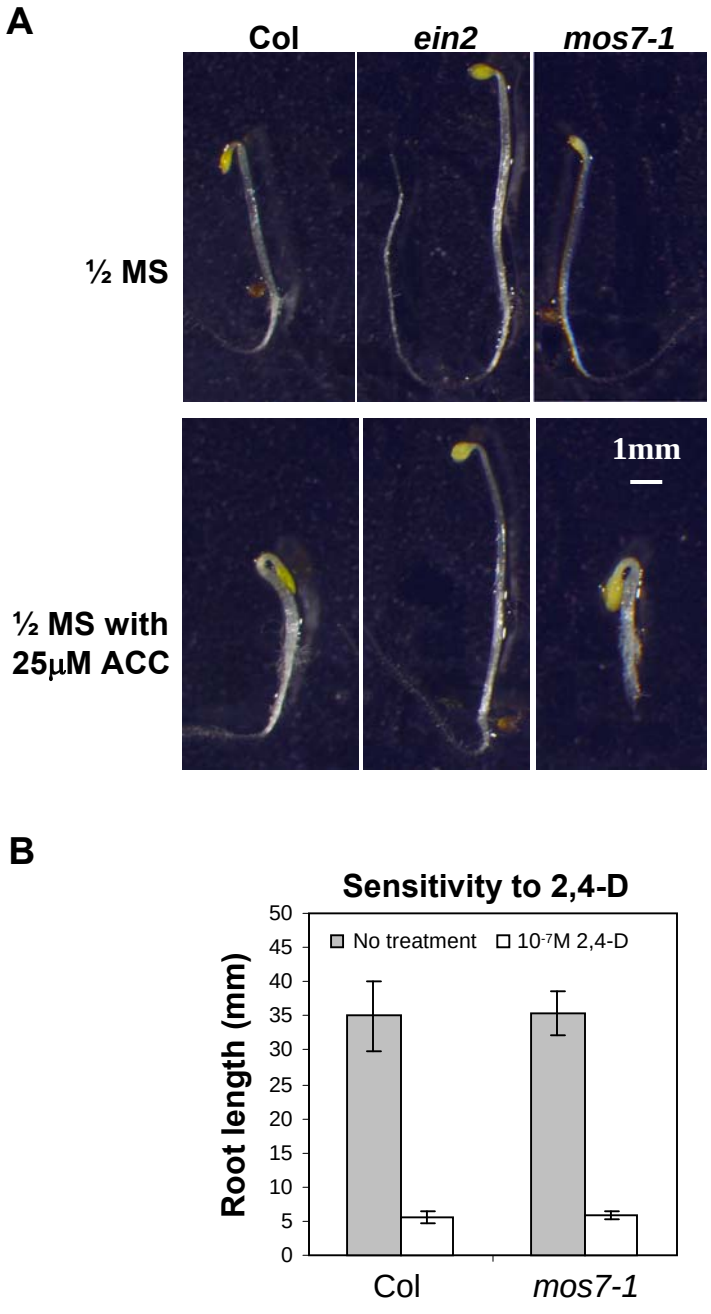

Supplementary Figure 5. Hormonal assays on *mos7-1*.
(A) Sensitivity of indicated genotypes to 25μM ACC (1-Aminocyclopropanecarboxylic acid). Seeds were sown on the specified plates and vernalized in the dark at 4°C for 72 h. The plates were placed in constant white light at 22°C for 6 hr and then placed in the dark at 22°C maintaining the same orientation and allowed to grow vertically for 3 more days.
(B) Sensitivity to the auxin analog, 2,4-D (2,4-Dichlorophenoxyacetic acid). Seeds were first sown on ½MS plates and cold treat for 72h. Seeds were allowed to germinate for 3 days on ½MS plates and transferred to specified plates. Root lengths were measured 7 days after germination.

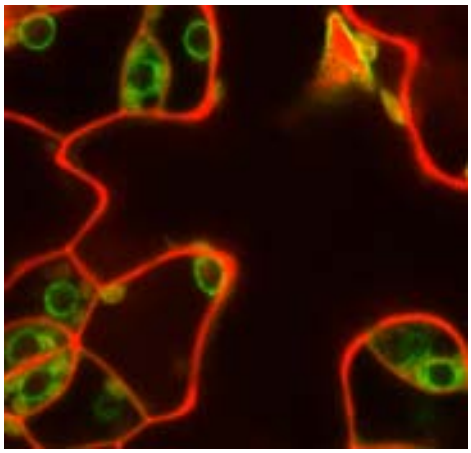

35S::mos7-1-GFP

Supplementary Figure 6. Subcellular localization of mos7-1-GFP fusion proteins in leaf pavement cells. Plant cell walls were stained with 5mg/ml propidium iodine (red).

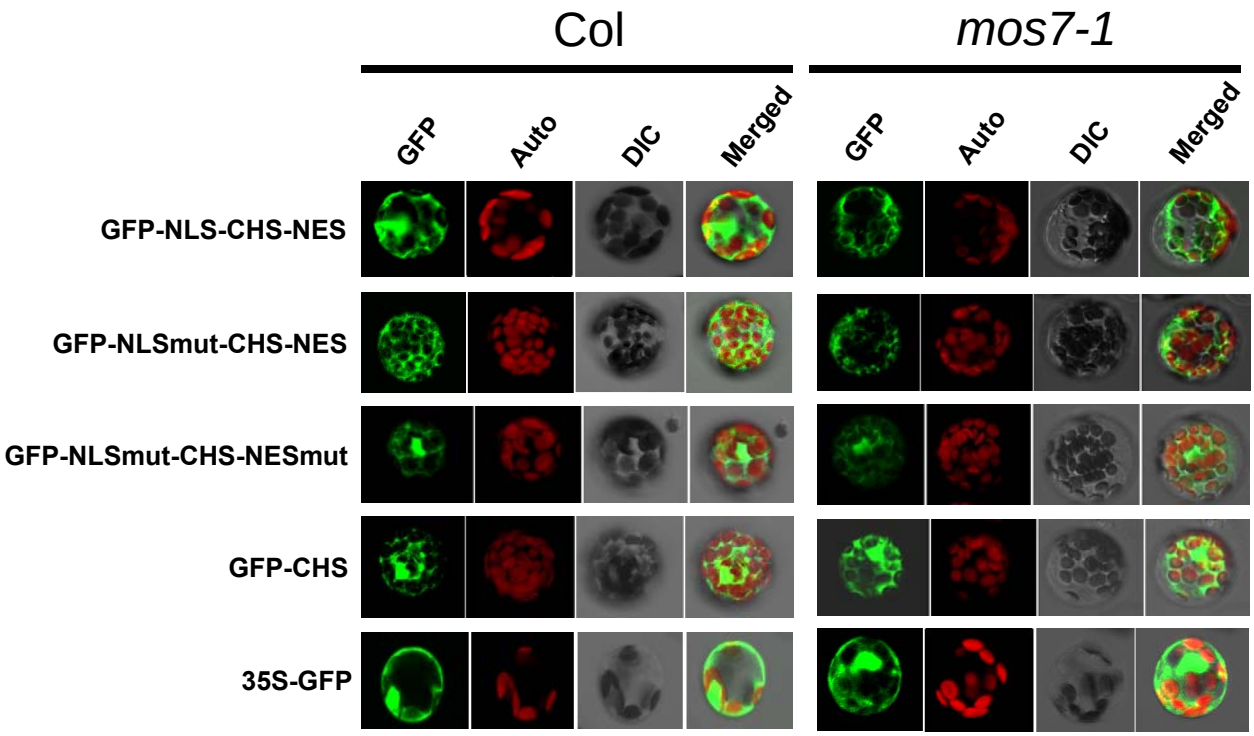

Supplementary Figure 7. *In vivo* nuclear transport assay of chalcone synthase (CHS) fused to GFP.

Arabidopsis protoplast were transiently transformed with CHS-GFP constructs (Haasen et al., 1999) and analyzed for GFP localization by confocal microscopy.

Cheng_Sup Fig8

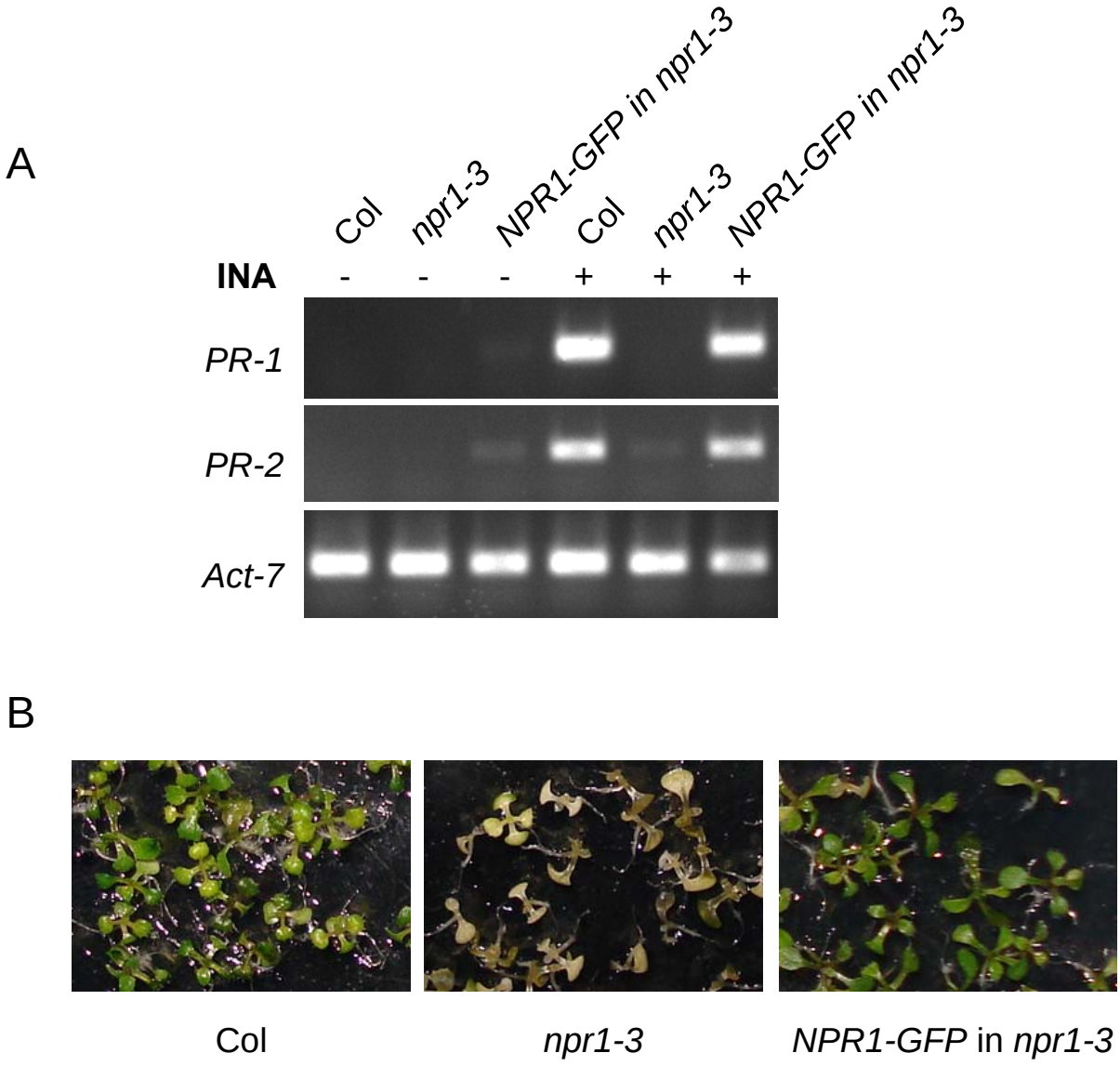

Supplementary Figure 8. Complementation of *npr1-3* by *NPR1-GFP* expressed under the control of its native promoter

(A) *PR* gene expression in the indicated genotypes. Total RNA was prepared from three week-old plants grown on MS medium in the presence (+) or absence (-) of 50 μ M INA and reverse transcribed to obtain total cDNA. The cDNA samples were normalized by real-time PCR using *Actin7* (Act-7F: GGTGTCATGGTTGGTATGGGTC and Act-7R: CCTCTGTGAGTAGAACTGGGTGC). *PR-1*, *PR-2*, and *Actin7* were amplified by 28, 30 and 30 cycles of PCR, respectively, using equal amounts of total cDNA and the products were analyzed by agarose gel electrophoresis with ethidium bromide staining.

(B) Tolerance of Col, *npr1-3*, and *npr1-3* transformed with *NPR1-GFP* to high concentrations of SA. Seeds were plated on MS medium containing 0.2 mM SA and the pictures were taken 10 days post germination.

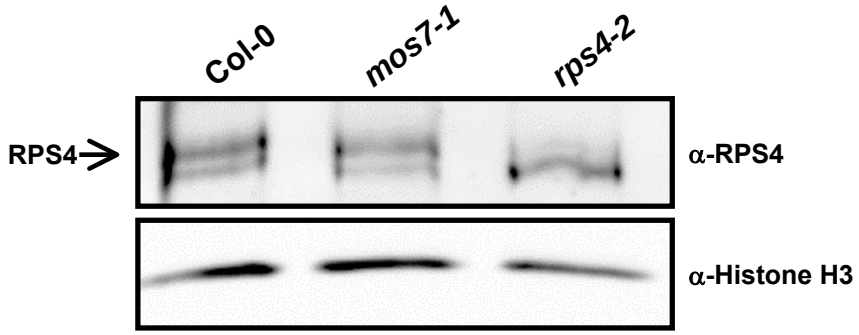

Supplementary Figure 9. Nuclear RPS4 in *mos7-1*.
Immunoblot analysis of RPS4 in nuclear protein extracts of unchallenged leaf tissues. Equal loading was monitored by probing the membrane with anti-Histone H3.